Attractive Channel Skyrmions and the Deuteron

R.A. Leese

Mathematical Institute

24-29 St. Giles

Oxford OX1 3LB, UK

e-mail: leese@maths.ox.ac.uk

N.S. Manton

Department of Applied Mathematics and Theoretical Physics

Silver Street

Cambridge CB3 9EW, UK

e-mail: nsm10@amtp.cam.ac.uk

B.J. Schroers

Department of Mathematical Sciences

South Road

Durham DH1 3LE, UK

e-mail: b.j.schroers@durham.ac.uk

Abstract

The deuteron is described as a quantum state on a ten-dimensional manifold M_{10} of Skyrme fields of degree two, which are obtained by calculating the holonomy of $SU(2)$ instantons. The manifold M_{10} includes both toroidal configurations of minimal energy and configurations which are approximately the product of two Skyrmions in the most attractive relative orientation. The quantum Hamiltonian is of the form $-\Delta + V$, where Δ is the covariant Laplace operator on M_{10} and V is the potential which M_{10} inherits from the Skyrme potential energy functional. Quantum states are complex-valued functions on the double cover of M_{10} satisfying certain constraints. There is a unique bound state with the quantum numbers of the deuteron, and its binding energy is approximately 6 MeV. Some of the deuteron's electrostatic and magnetostatic properties are also calculated and compared with experiment.

1   Introduction

A fundamental challenge in particle physics is to understand nuclear forces from first principles. So far, there is no quantitative understanding of nuclear binding starting with quarks and QCD, but one may attempt to investigate nuclei in terms of an effective low energy theory, like the Skyrme model [1]. In the Skyrme model, nucleons are solitons, and the parameters of the model are fixed so that the masses of the nucleon and the delta resonance are in agreement with experiment. All of nuclear physics can in principle then be derived from the Skyrme model (assuming that it is at least approximately right).

Further simplifications are necessary to make progress with this programme. It is generally agreed that treating the Skyrme model as a quantum field theory is very hard, and to study nucleons and their interactions one needs to reduce the Skyrme model to a finite-dimensional quantum mechanics. This can be done by picking out, as naturally as possible, a $6N$-dimensional set of Skyrme fields to model N nucleons. One nucleon is a quantised state of a Skyrmion, the lowest energy classical configuration with unit baryon number. The Skyrmion has six classical degrees of freedom - three translational and three rotational - and their quantisation gives a nucleon with momentum and correlated spin and isospin. There are various suggestions for a twelve-dimensional set M_{12} of two-Skyrmion fields. All include the product of two well-separated single Skyrmions (as suggested by Skyrme in [2]) to model well-separated nucleons, but it has been known for years that the product ansatz is not good for Skyrmions close together. The minimal energy two-Skyrmion fields are configurations with toroidal symmetry in which two separated Skyrmions have coalesced. These should be included in M_{12}.

The idea we favour, in principle, is to define M_{12} as the unstable manifold of the hedgehog two-Skyrmion configuration. This is discussed in detail in [3]. There is a quantum Hamiltonian for the motion on M_{12}, of the form $H = -\Delta + V$, where Δ is the Laplacian on M_{12} and V is the potential energy. In this paper we do not consider this Hamiltonian, but a further simplification. It is known that M_{12} has two naturally defined, low-lying submanifolds, which should be most important for low-energy physics of two nucleons. The first, denoted M_8, is eight-dimensional and consists of the toroidal configurations of minimal energy. Braaten and Carson considered the quantum mechanics on M_8 in [4]. They calculated the Hamiltonian and found the lowest energy stationary state compatible with the nucleons being treated as fermions. This state is identified with the deuteron. Not surprisingly, Braaten and Carson found a very large binding energy, and a small physical size. This is because the Skyrmions are not allowed to explore the full twelve-dimensional M_{12}, but only the eight-dimensional M_8. Nevertheless, Braaten and Carson's analysis is very instructive and is an important inspiration for our work.

We have considered the quantisation on a ten-dimensional submanifold M_{10} of M_{12}. Again the Hamiltonian is derived from the kinetic and potential parts of the Skyrme model Lagrangian, restricted to the fields in M_{10}. The manifold M_{10} is the set of attractive channel fields, which is a low-lying valley in M_{12}. It can be defined by taking two well-separated Skyrmions, oriented so that they maximally attract (i.e. one is rotated by π relative to the other, with the axis of rotation orthogonal to the line joining them), and allowing them to approach until they coalesce into a toroidal configuration. Ideally one would follow a gradient flow curve, or a path of steepest descent. The ten coordinates of M_{10} are accounted for by the separation parameter, overall translations, rotations and iso-rotations. M_{10} should be thought of as the smallest subset of M_{12} which includes Skyrmion separation.

In practice, we have not followed the prescription above for constructing M_{10}. Instead, we have defined an approximation to M_{10} consisting of Skyrme fields generated by Yang-Mills instantons. The details of the construction are explained in section 3. The instanton approach has some advantages which compensate for the fact that the fields do not have quite as low energies as those obtained by gradient flow. The main advantage is that the fields and their currents can be calculated by numerical integration of ordinary differential equations, whereas the gradient flow approach requires the numerical solution of a partial differential equation. Also, there is an explicit separation parameter ρ in the instanton data, which is a convenience. A disadvantage of the instanton approach is that it requires the pions to be regarded as massless. Other approaches can deal with pions which have their physical mass. It would certainly be worthwhile to work with M_{10} as defined by the gradient flow, and compare with the results here.

It is worth comparing the picture of the two nucleon interaction that emerges from the Skyrme model with conventional nuclear potential models. The basic difference is that no subset of the coordinates on M_{10} can be identified simply with the positions of the two nucleons. While the two Skyrmions are separated one can identify two points where the energy density (or baryon number density) is maximal, but when they coalesce these points disappear as the Skyrmions lose their identities. The energy density of a toroidal configuration is maximal on a circle. Related to this is the fact that, in the attractive channel, two Skyrmions are never closer together than in a toroidal configuration, and we shall define below a separation parameter ρ lying in the range $[\rho_0, \infty]$, where ρ_0 corresponds to the toroidal configurations, and is positive. When Skyrmions approach head-on they pass through a toroidal configuration, scatter through 90° and separate again. The radial part of the deuteron wavefunction $u(\rho)$ satisfies a radial Schrödinger equation on the interval $[\rho_0, \infty)$. Since M_{10} is smooth at ρ_0, the boundary condition there is that u is finite and $du/d\rho = 0$. In fact, $u(\rho)$ is maximal at ρ_0, which is where not only the potential V, but even the effective potential V_{eff} occurring in the radial equation is deepest. This is quite

different from a point-particle description of nucleons where a hard core potential is required to keep the nucleons from being close together. With a hard core, the boundary condition is $u(0) = 0$, or if the core potential is infinite for $\rho < \rho_1$, then $u(\rho_1) = 0$. In this situation, the wavefunction is usually maximal outside the point where the potential is deepest. As a consequence, a stronger attraction is needed to compensate. The Skyrme model seems to solve the usual problem of a 'medium range central attraction' through the geometry of M_{10}.

As an aside, we point out that the quantisation of a ten-dimensional family of two-Skyrmions was also considered in [5]. The ten-dimensional family, like our manifold M_{10}, was obtained by acting with translations, rotations and iso-rotations on a one-parameter family of fields which interpolates between the toroidal configuration and two-Skyrmions which are approximately of the product form, but have additional reflection symmetries. These reflection symmetries also play a role in our analysis, but our quantisation scheme differs from that of [5], which appears incorrect. In [5] an effective radial potential between Skyrmions was calculated on the interval $[0, \infty)$. The wavefunction was required to vanish at $\rho = 0$, and there was (by a long way) no bound state. We find a bound state with a very similar potential because of our different (and we believe correct) boundary conditions.

There is well-defined angular momentum in our formalism, but because the Skyrmions are extended objects and interact, there is no well-defined split into orbital and spin parts of the angular momentum. Consequently we cannot perform the usual decomposition of the deuteron wavefunction into s-wave and d-wave parts. Nevertheless we can calculate physical quantities related to this splitting, like the electric quadrupole moment.

The paper is organised as follows. Section 2 contains a review of the Skyrme model and its symmetries. In section 3 we review how Skyrme fields are obtained from instantons, and in particular how 2-Skyrmion attractive channel fields are obtained and parametrised. Section 4 describes the topological structure and the symmetries of the manifold M_{10}. The form of the Skyrme Lagrangian restricted to attractive channel fields is described in section 5. The Lagrangian depends on nine functions of the Skyrmion separation parameter ρ. These are calculated numerically, but for large values of ρ we also have analytic formulae, which provide a useful check. The appendix contains details of the numerical methods used. In section 6, the quantum Hamiltonian in the attractive channel is derived from the Lagrangian, and it is explained, using angular momentum analysis, how the stationary Schrödinger equation reduces to a radial equation. The bound states of this radial equation are discussed in section 7, and the lowest physically allowed state is identified with the deuteron. In section 8, various physical properties of our deuteron state are calculated and compared with the values obtained by Braaten and Carson, and with experiment. Some of the results are satisfactory, others less so. For the first time a sensible binding energy of order 5 MeV is obtained in a Skyrme model calculation. The deuteron has the right size, too, but its electric

quadrupole moment is too large and its magnetic dipole moment is too small. We conclude, in section 9, with some remarks on how one might correct our calculations on M_{10} without going to a full quantisation on the manifold M_{12}. Ideally, however, quantum mechanics on M_{12} is what should be done next.

2   The Skyrme Model

We set the speed of light to 1 and use the metric diag(1,-1,-,1,-1) on Minkowski space. Points in Minkowski space are written as $(t, \boldsymbol{x})$ with coordinates x^μ, $\mu = 0, 1, 2, 3$, and the Einstein summation convention is used throughout. The basic field of the Skyrme model is the $SU(2)$-valued field $U(t, \boldsymbol{x})$, which can also be expressed in terms of the pion fields:

$$U(t, \boldsymbol{x}) = \sigma(t, \boldsymbol{x}) + i\boldsymbol{\pi}(t, \boldsymbol{x})\cdot\boldsymbol{\tau} \tag{2.1}$$

where τ_1, τ_2, τ_3 are the Pauli matrices and $\sigma^2 + \boldsymbol{\pi}^2 = 1$. The equations of motion for U are the Euler-Lagrange equations derived from the Lagrangian density

$$\mathcal{L} = -\frac{F_\pi^2}{16}\text{tr}(R_\mu R^\mu) + \frac{1}{32e^2}\text{tr}([R_\mu, R_\nu][R^\mu, R^\nu]). \tag{2.2}$$

The right-currents R_μ are defined via

$$R_\mu = (\partial_\mu U)U^\dagger, \tag{2.3}$$

where ∂_μ denotes partial differentiation with respect to x_μ. The constants F_π and e are free parameters of the Skyrme model. We found it convenient to remove them from our calculations by using $F_\pi/4e$ as the unit of energy and $2/eF_\pi$ as the unit of length. Thus we work in geometrical units, and the Lagrangian density takes the form

$$\mathcal{L} = -\frac{1}{2}\text{tr}(R_\mu R^\mu) + \frac{1}{16}\text{tr}([R_\mu, R_\nu][R^\mu, R^\nu]). \tag{2.4}$$

The parameters F_π and e can be fixed in a number of ways. Most authors adopt the approach of [6] and [7] where F_π and e are tuned to reproduce the masses of the proton and the delta resonance without and with the physical pion mass respectively. All papers written so far on the deuteron in the Skyrme model take into account the physical pion mass and use the set of parameters given in [7]. For ease of comparison we will follow that practice, although the pion mass is assumed to be zero here. Thus, with the values of F_π and e as in [7], our units are related to conventional units via

$$\frac{F_\pi}{4e} = 5.58\,\text{MeV} \qquad \text{and} \qquad \frac{2}{eF_\pi} = 0.755\,\text{fm}. \tag{2.5}$$

Since

$$\hbar = 197.3\text{MeV fm} = 46.8\left(\frac{F_\pi}{4e}\right)\left(\frac{2}{eF_\pi}\right), \tag{2.6}$$

5

it follows that, in our units where $F_\pi/4e = 2/eF_\pi = 1$, $\hbar = 46.8$.

It is useful to think of the Skyrme model as an infinite-dimensional Lagrangian system whose configuration space Q is the space of maps

$$U : \mathbf{R}^3 \mapsto SU(2) \tag{2.7}$$

which obey

$$\lim_{|\boldsymbol{x}| \to \infty} U(\boldsymbol{x}) = \mathbf{1}_2. \tag{2.8}$$

The Lagrangian $L = \int d^3x \mathcal{L}$ has the usual form $L = T - V$, where the T is the kinetic energy

$$T = \int d^3x \left\{ -\frac{1}{2}\text{tr}(R_0 R_0) - \frac{1}{8}\text{tr}([R_i, R_0][R_i, R_0]) \right\} \tag{2.9}$$

and V is the potential energy

$$V = \int d^3x \left\{ -\frac{1}{2}\text{tr}(R_i R_i) - \frac{1}{16}\text{tr}([R_i, R_j][R_i, R_j]) \right\}. \tag{2.10}$$

The condition (2.8) is imposed in order to ensure that the elements of Q have finite energy. It is important topologically because it allows one to compactify $\mathbf{R}^3$ to S^3 and to regard an element U of Q as a map $S^3 \mapsto SU(2) \cong S^3$. Thus $\pi_0(Q) = \pi_3(S^3) = \mathbf{Z}$, showing that Q is not connected but has components Q_B labelled by an integer B which is the degree of any element of Q_B. Physically, the integer B is interpreted as the baryon number of a Skyrme field. It can be calculated by integrating the zeroth component of the (conserved) baryon number current

$$B^\mu = \frac{\epsilon^{\mu\nu\alpha\beta}}{24\pi^2}\text{tr}(R_\nu R_\alpha R_\beta), \tag{2.11}$$

where we use the convention $\epsilon_{0123} = -\epsilon^{0123} = 1$. Thus,

$$B^0 = -B_0 = -\frac{\epsilon_{ijk}}{24\pi^2}\text{tr}(R_i R_j R_k) = -\frac{1}{8\pi^2}\text{tr}([R_1, R_2]R_3) \tag{2.12}$$

and

$$B^i = B_i = \frac{\epsilon_{ijk}}{8\pi^2}\text{tr}(R_j R_k R_0). \tag{2.13}$$

Then the baryon number is

$$B = \int d^3x B^0. \tag{2.14}$$

The fundamental group of Q is also important here. In general, the fundamental group of a space depends on the choice of a base point, but it is explained in [8] that

$$\pi_1(Q) = \pi_1(Q_B) = \mathbf{Z}_2 \tag{2.15}$$

6

for any $B \in \mathbf{Z}$. The group $\pi_1(Q)$ is generated by the rotation of a single Skyrmion by 2π. More generally, it is shown in [8] that the loop generated by rotating an element of Q_B by 2π is contractible if B is even and not contractible if B is odd. A further important topological result, due to Finkelstein and Rubinstein [9], is that the rotation of one Skyrmion by 2π and the exchange of two Skyrmions are homotopic paths in Q_B, for $|B| \geq 2$.

We will use the following conventions when describing Skyrme fields. We refer to the domain $\mathbf{R}^3$ of a static Skyrme field as physical space and to the range $SU(2)$ as iso-space. We write $\{e_1, e_2, e_3\}$ for the canonical orthonormal basis of $\mathbf{R}^3$ ($e_1 = (1,0,0)$ etc.) and in the decomposition (2.1) of elements of $SU(2)$ we refer to $i\tau_a$ ($a = 1,2,3$) as the a-th axis in iso-space. G stands for an $SU(2)$ matrix and $D(G)$ for the $SO(3)$ matrix associated to G via

$$D(G)_{ab} = \tfrac{1}{2}\mathrm{tr}(\tau_a G \tau_b G^\dagger). \tag{2.16}$$

For fixed B, the symmetry group of the Lagrangian system with configuration space Q_B and Lagrangian L is

$$P \times SO(3)^I \times E_3. \tag{2.17}$$

Here P is the combined parity operation in space and iso-space,

$$P : U(\boldsymbol{x}) \mapsto U^\dagger(-\boldsymbol{x}), \tag{2.18}$$

and $SO(3)^I$ is the group of iso-rotations. Its action can be written in terms of an $SU(2)$ matrix C as

$$U(\boldsymbol{x}) \mapsto CU(\boldsymbol{x})C^\dagger \tag{2.19}$$

or, in terms of the pion fields,

$$\boldsymbol{\pi}(\boldsymbol{x}) \mapsto D(C)\boldsymbol{\pi}(\boldsymbol{x}). \tag{2.20}$$

Finally, the euclidean group E_3 is the semidirect product of the spatial rotation group $SO(3)^J$ and the group $\mathbf{R}^3$ of translations. An element $(D(G), \boldsymbol{S}) \in E_3$ acts on a vector $\boldsymbol{x}$ according to

$$\boldsymbol{x} \mapsto D(G)\boldsymbol{x} + \boldsymbol{S} \tag{2.21}$$

and on Skyrme fields via pull-back:

$$U(\boldsymbol{x}) \mapsto U(D(G)^{-1}(\boldsymbol{x} - \boldsymbol{S})). \tag{2.22}$$

The group (2.17) has discrete subgroups which will be important for us. We therefore introduce the notation O_{ai} ($a, i \in 1,2,3$) for simultaneous rotations by π around the a-th

axis in iso-space and the i-th axis in physical space. It will also be useful to write O_{0i} for the rotation by π about the i-th axis in physical space only and O_{a0} for the rotation by π about the a-th axis in iso-space only. Finally we define hyperplane reflections in space and iso-space $P_{ai} = PO_{ai}$.

For the discussion of the kinetic energy we need carefully to define angular velocities: the left-invariant or body-fixed angular velocity for spatial rotations $\boldsymbol{\omega}$ is defined via

$$\boldsymbol{\omega}\cdot\boldsymbol{t} = G^{\dagger}\dot{G}, \tag{2.23}$$

where $t_i = -\frac{i}{2}\tau_i$ (so that $[t_i, t_j] = \varepsilon_{ijk}t_k$) and the dot denotes differentiation with respect to time. Equivalently, in terms of $D(G)$:

$$\boldsymbol{\omega}\cdot\boldsymbol{s} = D(G)^{-1}\dot{D}(G), \tag{2.24}$$

where the s_i are 3×3 matrices with components $(s_i)_{jk} = -\varepsilon_{ijk}$. They also satisfy $[s_i, s_j] = \varepsilon_{ijk}s_k$. The corresponding right-invariant or space-fixed angular velocity is less important for us; it is given by $D(G)\boldsymbol{\omega}$.

Similarly one defines the body-fixed angular velocity $\boldsymbol{\Omega}$ for iso-rotations via

$$\boldsymbol{\Omega}\cdot\boldsymbol{t} = C^{\dagger}\dot{C}. \tag{2.25}$$

The corresponding space-fixed angular velocity is again given by $D(C)\boldsymbol{\Omega}$. The angular momenta associated to the angular velocities in space and iso-space will be discussed in section 6.

3   Attractive Channel Skyrme Fields from Instantons

The idea that Skyrme fields can be generated from Yang-Mills instantons was proposed in [10] and subsequently developed in a number of papers, including [11] and [12]. The attractive channel fields generated from instantons were also studied in [13].

Briefly, consider the fourth component A_4 of a self-dual $SU(2)$ Yang-Mills field, or instanton, on $\mathbf{R}^4$, and define the holonomy along all lines parallel to the x_4-axis

$$U(\boldsymbol{x}) = \mathcal{P}\exp - \int_{-\infty}^{\infty} A_4(\boldsymbol{x}, x_4)dx_4 \tag{3.1}$$

(the right hand side is a path-ordered exponential). The formula (3.1) defines an $SU(2)$-valued field which can be regarded as a Skyrme field on $\mathbf{R}^3$. Provided A_4 decays sufficiently rapidly as $|\boldsymbol{x}| \to \infty$, $U(\boldsymbol{x})$ satisfies the asymptotic condition (2.8). Moreover, the degree, or baryon number of U equals the instanton number or charge [12].

The expression (3.1) is formal. It is computed by solving the differential equation

$$\partial_4 \tilde{U} = -A_4 \tilde{U}, \tag{3.2}$$

where $\tilde{U}$ is defined on $\mathbf{R}^4$. One imposes the boundary condition

$$\lim_{x_4 \to -\infty} \tilde{U}(\boldsymbol{x}, x_4) = \mathbf{1}_2 \tag{3.3}$$

and defines the Skyrme field $U(\boldsymbol{x})$ via

$$U(\boldsymbol{x}) = \lim_{x_4 \to \infty} \tilde{U}(\boldsymbol{x}, x_4). \tag{3.4}$$

For details of the numerical implementation of these steps we refer the reader to the appendix, and also [23].

The simplest Skyrme field one obtains this way (apart from the vacuum) is the hedgehog Skyrme field of degree 1. This is generated by a unit charge instanton centred at the origin. As shown in [10] the equation (3.2) can be solved analytically in this case, and gives the Skyrme field

$$U_H(\boldsymbol{x}) = \exp i f(r)\hat{\boldsymbol{x}} \cdot \boldsymbol{\tau} \tag{3.5}$$

where

$$f(r) = \pi \left(1 - (1 + \frac{\lambda}{r^2})^{-\frac{1}{2}} \right). \tag{3.6}$$

The scale parameter λ is chosen to minimise the energy of the field, which is interpreted as the Skyrmion mass. The minimum is obtained for $\lambda = 2.11$; Then the mass is $M = 1.243 \cdot 12\pi^2 = 147.2$ and the moment of inertia is $\Lambda = 8.363 \cdot 16\pi/3 = 140.1$ (normalised so that the kinetic energy of a hedgehog spinning with frequency ω is $\frac{1}{2}\Lambda\omega^2$). Using the formula $M + 3\hbar^2/8\Lambda$ [6], it follows that the prediction for the nucleon mass is $M = 153.1$, which is 854.1 MeV in physical units. This rather small value results from the combination of the instanton generated profile function (3.6) with the choice of units (2.5) designed to reproduce the experimental values for the nucleon and delta masses when the physical pion mass is taken into account. However, the absolute value of the nucleon mass (and later the deuteron mass) is not important here. We are mainly interested in the deuteron's binding energy, which is the difference between its own mass and the mass of two free nucleons. For later use we also note that f has the simple form

$$f(r) \sim \frac{p}{r^2} \tag{3.7}$$

when r is large. The constant p (which may be interpreted as the Skyrmion's pion dipole strength) is $\pi\lambda/2$.

The attractive channel two-Skyrmion fields, generated by instantons, were discussed in detail in [12]. There is also an analytic formula for A_4, given by Jackiw, Nohl and Rebbi (JNR) in [14], but the equation (3.2), which gives the Skyrme fields, must still be solved numerically. The JNR formula is somewhat gauge dependent and ungeometrical, so before giving it we recall Hartshorne's geometrical description of charge two instantons. Hartshorne showed that associated to any charge two $SU(2)$ instanton in $\mathbf{R}^4$ there is a circle and an ellipse in $\mathbf{R}^4$ (the circle can degenerate to a straight line but this will not be relevant here). The ellipse is in the same plane as the circle, and interior to it. Moreover, the ellipse satisfies the Poncelet condition; that is, there exists a triangle with vertices on the circle whose sides are tangent to the ellipse. Poncelet's theorem states that if one such triangle exists, then there are infinitely many and any point on the circle can be taken as one vertex.

Two well-separated Skyrmions maximally attract if one is rotated relative to the other by π about a line perpendicular to the line joining them. The attractive channel interpolates between such Skyrmion pairs and the toroidal two-Skyrmion, where the Skyrmions coalesce into the minimal energy configuration. The attractive channel is modelled by a subset of the Skyrme fields generated by charge two instantons. This is the subset where the Hartshorne circle lies in a spatial plane in $\mathbf{R}^4$ (orthogonal to the x_4-axis) and where the ellipse is concentric with the circle. Without loss of generality, we may suppose the common centre is at the origin in $\mathbf{R^4}$, that the circle is in the x_1x_2-plane, and that the ellipse has its major axis along the 1-axis, see figure 1. In this standard form there are two parameters in the Hartshorne data for attractive channel fields. These may be taken to be the radius L of the circle and the length L_1 of the semi-major axis of the ellipse. We denote the length of the semi-minor axis by L_2. The Poncelet condition is that $L_1 + L_2 = L$. The configuration in figure 1 is rather symmetric, and this manifests itself in the symmetries of the corresponding Skyrme fields, which we will discuss in section 4.

When $L_1 \gg L_2$, the instanton associated with the circle and ellipse of figure 1 generates a Skyrme field consisting of two well-separated Skyrmions, centred near the ends of the ellipse (the x_4-coordinate is irrelevant now). When $L_1 = L_2 = \frac{1}{2}L$, the ellipse becomes a circle, so there is higher symmetry, and the instanton generates a toroidal Skyrme field.

To progress, we need the explicit JNR formula for A_4 for the instantons whose Hartshorne data is as in figure 1. To this end we choose one triangle of the Poncelet porism; following Hosaka *et al.* [13] we choose the isosceles triangle shown. The JNR data consists of the points X_1, X_2, X_3 in $\mathbf{R}^4$ as shown and associated weights $\lambda_1, \lambda_2, \lambda_3$. These can be rescaled so that $\lambda_2 = \lambda_3 = 1$. It is natural to define the angle $\vartheta = \arcsin(1/(1+\lambda_1))$, whose geometrical significance is shown in figure 1. In JNR terms, the essential parameters of the instantons are the radius L of the circle and the angle ϑ, which lies in the range $(0, \frac{\pi}{6}]$. The semi-major axis of the ellipse is then $L_1 = (1 - \sin \vartheta)L$. The JNR gauge potential in $\mathbf{R}^4$ has a fourth

component of the form

$$A_4 = \tfrac{i}{2} \partial_i \ln \nu(x) \tau_i, \tag{3.8}$$

where ν is the following function of $x = (\boldsymbol{x}, x_4) \in \mathbf{R}^4$:

$$\nu(x) = \sum_{n=1}^{3} \frac{\lambda_n}{|x - X_n|^2}. \tag{3.9}$$

There is a slight technical complication in that the JNR gauge potentials do not decay sufficiently rapidly at large distances to extend smoothly from $\mathbf{R}^4$ to S^4; it turns out that an extra factor of -1 must be attached to U in (3.4), see also [12]. The Skyrme fields in the attractive channel are then given by (3.2) - (3.4).

The Hartshorne data in the standard form described above have two parameters, L and ϑ, and acting with spatial translations, rotations and iso-rotations on the Skyrme fields generated from the corresponding instantons one obtains an eleven-dimensional family of Skyrme fields, which is not desired. Instead of retaining L and ϑ as independent parameters we therefore fix L, for each value of ϑ, to the value which minimises the Skyrme potential energy. This fixes the scale of the Skyrmions in the configuration, so that for $\vartheta \approx 0$ we obtain the product of two well-separated hedgehog Skyrmions with the scale factor $\lambda = 2.11$ as in (3.6) and oriented so that the attraction is maximal. In the limit $\vartheta \to 0$, the energy of this configuration tends to $2M = 294.4$, twice the energy of a hedgehog Skyrmion. For $\vartheta = \pi/6$ we obtain a toroidal Skyrme field whose energy is $1.19 \cdot 24\pi^2 = 282.0$.

As a separation parameter we shall use $\rho = 2L(1 - \sin \vartheta) = 2L_1$. This makes physical sense: ρ is positive when $\vartheta = \pi/6$, taking the value $\rho_0 = 1.71$, and it tends to infinity as $\vartheta \to 0$. For small ϑ, ρ is an accurate estimate of the distance between the Skyrmion centres (for example, $2L$ is not so good). The field approaches a product of hedgehog fields with this separation, as can be seen by considering another triangle in the Poncelet porism, namely one which is isosceles and has one vertex on the 1-axis (see also [12]). Mathematically, our definition of separation is a little awkward, as L is a function of ϑ which is determined numerically, but this causes few problems in practice.

To sum up, starting with the standard Hartshorne data depicted in figure 1 we generate a 1-parameter family of attractive channel Skyrme fields in standard orientation, which we denote by $\hat{U}(\rho, \boldsymbol{x})$. The iso-orientation of $\hat{U}(\rho, \boldsymbol{x})$ is chosen so that for large ρ it is approximately a product of two well-separated hedgehog Skyrmions on the 1-axis with one hedgehog rotated relative to the other by π about the 3-axis:

$$\hat{U}(\rho, \boldsymbol{x}) \approx U_H(\boldsymbol{x} + \tfrac{1}{2}\rho\boldsymbol{e}_1)\tau_3 U_H(\boldsymbol{x} - \tfrac{1}{2}\rho\boldsymbol{e}_1)\tau_3. \tag{3.10}$$

When $\rho = \rho_0$, $\hat{U}(\rho, \boldsymbol{x})$ is the toroidal Skyrme field, centred at the origin and with the axis of the torus along the 3-axis.

4 Topology and Symmetries of the Manifold of Attractive Channel Fields

We define the manifold M_{10} of attractive channel fields as the orbit of the family of standard fields $\hat{U}(\rho, \boldsymbol{x})$ under the symmetry group (2.17). For most of this paper we will not be concerned with overall translations of the standard field $\hat{U}(\rho, \boldsymbol{x})$. Thus we also define the manifold M_7 of centred attractive channel fields as the quotient of M_{10} by the translation group $\mathbf{R}^3$. Alternatively one can think of M_7 as the orbit of the family of standard fields $\hat{U}(\rho, \boldsymbol{x})$ under

$$\mathcal{G} = SO(3)^I \times SO(3)^J \times P. \tag{4.1}$$

For fixed ρ, the orbit is diffeomorphic to the quotient of $\mathcal{G}$ by the isotropy group of its action on $\hat{U}(\rho, \boldsymbol{x})$.

The isotropy group consists, by definition, of all elements of $\mathcal{G}$ which leave $\hat{U}(\rho, \boldsymbol{x})$ invariant. The standard Hartshorne data in figure 1 is clearly invariant under reflections in the x_1x_2, x_2x_3 and x_1x_3 planes, but the Skyrme fields $\hat{U}(\rho, \boldsymbol{x})$ are only invariant under certain combinations of these reflections with reflections in iso-space. Explicitly these combinations are:

$$P_{21} : (\pi_1, \pi_2, \pi_3) \mapsto (\pi_1, -\pi_2, \pi_3) \quad \text{and} \quad (x_1, x_2, x_3) \mapsto (-x_1, x_2, x_3)$$
$$P_{22} : (\pi_1, \pi_2, \pi_3) \mapsto (\pi_1, -\pi_2, \pi_3) \quad \text{and} \quad (x_1, x_2, x_3) \mapsto (x_1, -x_2, x_3)$$
$$P_{33} : (\pi_1, \pi_2, \pi_3) \mapsto (\pi_1, \pi_2, -\pi_3) \quad \text{and} \quad (x_1, x_2, x_3) \mapsto (x_1, x_2, -x_3). \tag{4.2}$$

The group generated by these maps is an abelian subgroup of (2.17) of order 8 which we denote by $\mathcal{G}_8$. Its elements are

$$\mathcal{G}_8 = \{1, O_{11}, O_{12}, O_{03}, PO_{30}, P_{21}, P_{22}, P_{33}\}. \tag{4.3}$$

It is easy to check that

$$\text{Vier} = \{1, O_{11}, O_{12}, O_{03}\} \tag{4.4}$$

is a subgroup which is isomorphic to the viergruppe. Using

$$PO_{30}P_{21} = O_{11}$$
$$PO_{30}P_{22} = O_{12}$$
$$PO_{30}P_{33} = O_{03} \tag{4.5}$$

one shows further that there is an isomorphism

$$\mathcal{G}_8 \cong \text{Vier} \times \mathbf{Z}_2, \tag{4.6}$$

where $\mathbf{Z}_2 = \{1, -1\}$, which identifies $PO_{30} \in \mathcal{G}_8$ with $(1, -1) \in \text{Vier} \times \mathbf{Z}_2$. It follows that for $\rho > \rho_0$ the isotropy group of $\hat{U}(\rho, \boldsymbol{x})$ is $\mathcal{G}_8$ and that the orbit under $\mathcal{G}$ is diffeomorphic to

$$\left(SO(3)^I \times SO(3)^J\right) / \text{Vier}. \tag{4.7}$$

When $\rho = \rho_0$, there is an additional invariance. The field $\hat{U}(\rho_0, \boldsymbol{x})$ is invariant under spatial rotations about the 3-axis by some angle χ and simultaneous iso-rotation about the 3-axis by 2χ. Explicitly

$$e^{-i\chi\tau_3}\hat{U}(\rho_0, D(e^{\frac{i\chi}{2}\tau_3})\boldsymbol{x})e^{i\chi\tau_3} = \hat{U}(\rho_0, \boldsymbol{x}), \qquad \chi \in [0, 2\pi). \tag{4.8}$$

Such transformations form an $SO(2)$ subgroup of $SO(3)^I \times SO(3)^J$ which we denote by $\mathcal{H}$. It follows that the isotropy group of $\hat{U}(\rho_0, \boldsymbol{x})$ is the semi-direct product of $\mathcal{H}$ with the group consisting of $\{1, P_{22}, P_{33}, O_{11}\}$. Thus the orbit under $\mathcal{G}$ is diffeomorphic to

$$\left(SO(3)^I \times SO(3)^J\right) / O(2). \tag{4.9}$$

Here $O(2)$ is the semi-direct product of $\mathcal{H}$ with the group $\{1, O_{11}\}$. Note that the orbit under the action of $\mathcal{G}$ is six-dimensional if $\rho > \rho_0$ but only five-dimensional if $\rho = \rho_0$.

Concretely, any field in M_{10} can be written in terms of $SU(2)$ matrices C and G and a translation vector $\boldsymbol{S}$ as

$$C\hat{U}(\rho, D(G)^{-1}(\boldsymbol{x} - \boldsymbol{S}))C^\dagger. \tag{4.10}$$

For $\rho > \rho_0$, $D(C), D(G)$ and $\boldsymbol{S}$ can be used to parametrise the fields, but we should identify points related by the right action of O_{03} and O_{11}:

$$\begin{aligned} (D(C), D(G)) &\sim (D(C), D(G)O_{03}) \\ (D(C), D(G)) &\sim (D(C)O_{10}, D(G)O_{01}). \end{aligned} \tag{4.11}$$

It follows, as a consequence of the group structure, that points related by the right action of O_{12} are also identified. For $\rho = \rho_0$ we identify points related by the right action O_{11} and by the right action of elements in $\mathcal{H}$:

$$\begin{aligned} (D(C), D(G)) &\sim (D(C)O_{10}, D(G)O_{01}) \\ (D(C), D(G)) &\sim (D(Ce^{-i\chi\tau_3}), D(Ge^{-\frac{i\chi}{2}\tau_3})). \end{aligned} \tag{4.12}$$

The $\mathcal{G}$-orbit structure of M_7 can be used to coordinatise M_7 in terms of the separation parameter ρ and Euler angles (ϕ, θ, ψ) for $SO(3)^J$ and (α, β, γ) for $SO(3)^I$. More precisely we write an element $D(G)$ of $SO(3)^J$ as

$$D(G) = e^{\phi s_3}e^{\theta s_2}e^{\psi s_3} \tag{4.13}$$

where s_i are the generators of $SO(3)$ defined in section 2. Similarly an element $D(C)$ of $SO(3)^I$ can be written as

$$D(C) = e^{\alpha s_3} e^{\beta s_2} e^{\gamma s_3}. \tag{4.14}$$

The range of the Euler angles is $\phi, \psi, \alpha, \gamma \in [0, 2\pi)$ and $\theta, \beta \in [0, \pi)$. However, points related by the maps O_{03}, O_{11}, O_{12} should be identified. These maps now take the form

$$
\begin{aligned}
O_{03} : \quad & \beta \mapsto \beta, & \alpha \mapsto \alpha, & \quad \gamma \mapsto \gamma, \\
& \theta \mapsto \theta, & \phi \mapsto \phi, & \quad \psi \mapsto \psi + \pi \\
O_{11} : \quad & \beta \mapsto \pi - \beta, & \alpha \mapsto \alpha + \pi, & \quad \gamma \mapsto -\gamma, \\
& \theta \mapsto \pi - \theta, & \phi \mapsto \phi + \pi, & \quad \psi \mapsto -\psi \\
O_{12} : \quad & \beta \mapsto \pi - \beta, & \alpha \mapsto \alpha + \pi, & \quad \gamma \mapsto -\gamma, \\
& \theta \mapsto \pi - \theta, & \phi \mapsto \phi + \pi, & \quad \psi \mapsto \pi - \psi.
\end{aligned} \tag{4.15}
$$

Using the orbit structure of M_7 it is not difficult to understand its homotopy structure. This will be important in the quantum theory. All the results that are required here were already derived in [5], but it is useful to briefly state and prove them using our notation. Since M_7 is connected it is sufficient to consider paths which begin and end at the toroidal configuration $\hat{U}(\rho_0, \boldsymbol{x})$.

Our first claim is that loops generated by either spatial or iso-spatial rotations of $\hat{U}(\rho, \boldsymbol{x})$ by 2π are contractible in M_7. To see this we first note that rotations by 2π about any two axes are homotopic to each other; thus we can specify a convenient axis without loss of generality. The claim is clearly true for a loop generated by a spatial rotation of $\hat{U}(\rho_0, \boldsymbol{x})$ by 2π about the 3-axis, since such a rotation is equivalent to an iso-rotation by 4π about the 3-axis. Since rotations by 4π are homotopic to the identity the loop is contractible. To show the contractibility of the loop generated by an iso-rotation by 2π we also initially consider a rotation about the 3-axis. Then we smoothly increase ρ until $\hat{U}(\rho, \boldsymbol{x})$ is approximately the product of two well-separated hedgehog fields as in (3.10). Since the hedgehogs are rotated relative to each other about the 3-axis, iso-rotating the whole configuration by 2π about the 3-axis is the same as iso-rotating each of the hedgehogs by the same amount about the 3-axis. However, by our earlier remark this loop is homotopic to rotating each of hedgehogs by 2π about the 1-axis. Moreover, for hedgehogs iso-spatial rotations are the same as spatial rotations. Then, since the two hedgehogs are separated along the 1-axis, a spatial rotation of each by 2π about the 1-axis is equivalent to an overall spatial rotation by 2π about the 1-axis. The contractibility of the loop then follows from our earlier result that a spatial rotation by 2π is contractible.

Our second claim is that all loops in M_7 are either contractible or homotopic to a rotation of one of the hedgehog fields in the product ansatz (3.10). It then follows that $\pi_1(M_7) = \mathbf{Z}_2$, so M_7 has the same fundamental group as the space Q_2 of all Skyrme fields of degree 2. To

prove the claim we have to consider the paths which connect points identified by O_{03}, O_{11} and O_{12}. First consider the path Γ_{03} in M_7 obtained by performing a spatial rotation of $\hat{U}(\rho_0, \boldsymbol{x})$ by π about the 3-axis. The map O_{03} identifies the endpoint with the starting point, so the path is closed. However, for toroidal configurations a spatial rotation by π about the 3-axis is equivalent to an iso-rotation by 2π about the 3-axis. Hence the path is contractible by our first claim. The second path we consider is obtained by rotating $\hat{U}(\rho_0, \boldsymbol{x})$ in both space and iso-space by π about the 1-axes. This path, denoted Γ_{11}, is closed because the map O_{11} identifies the endpoint with the starting point. By increasing ρ so that $\hat{U}(\rho, \boldsymbol{x})$ is of the product form (3.10) this loop can be deformed into the following

$$e^{-\frac{i}{2}\chi\tau_1}U_H(D(e^{\frac{i}{2}\chi\tau_1})\boldsymbol{x} + \tfrac{1}{2}\rho\boldsymbol{e}_1))\tau_3 U_H(D(e^{\frac{i}{2}\chi\tau_1})\boldsymbol{x} - \tfrac{1}{2}\rho\boldsymbol{e}_1)\tau_3 e^{\frac{i}{2}\chi\tau_1}$$
$$= U_H(\boldsymbol{x} + \tfrac{1}{2}\rho\boldsymbol{e}_1))\tau_3 U_H(D(e^{i\chi\tau_1})\boldsymbol{x} - \tfrac{1}{2}\rho\boldsymbol{e}_1)\tau_3, \qquad \chi \in [0, \pi). \quad (4.16)$$

Hence it is homotopic to a rotation by 2π of one of the two Skyrmions in the product ansatz. We know that such a loop is not contractible in Q_2 and, a $fortiori$, it is not contractible in M_7. It follows also that the loop Γ_{11}^2 is homotopic to a rotation by 4π of one of the Skyrmions and hence contractible. Finally there is the loop Γ_{12} associated with the identification O_{12}. It is obtained by performing a spatial rotation by π about the 2-axis and an iso-rotation by π about the 1-axis. It follows from $O_{12} = O_{11}O_{03}$ that $\Gamma_{12} = \Gamma_{11}\Gamma_{03}$. Hence Γ_{12} is in the same homotopy class as Γ_{11} and not contractible.

To summarise, loops in M_7 are either contractible or homotopic to a rotation of one Skyrmion by 2π. Our discussion of the loops Γ_{11}, Γ_{03} and Γ_{12} suggests the following physical interpretation of the identifications O_{11}, O_{03} and O_{12} in the asymptotic region of M_7 which describes well-separated Skyrmions: O_{11} identifies configurations related by rotating one of the Skyrmions by 2π, O_{12} identifies configurations related by the exchange of the two Skyrmions and O_{03} identifies configurations related by the exchange of the two Skyrmions and the simultaneous rotation of each by π. As mentioned in section 2, the rotation of one Skyrmion and the exchange of two Skyrmions are homotopic paths in Q_2. We have seen that the two operations are also homotopic in M_7. Note, however, that the homotopy does not require the creation of a Skyrmion - anti-Skyrmion pair, as is often claimed. In fact, we have checked that the baryon density for all fields in M_7 is non-negative everywhere.

5   The Lagrangian in the Attractive Channel

The Lagrangian in the attractive channel is, by definition, the restriction of the Skyrme Lagrangian L to M_{10}. We call it L_{att}. The evaluation of potential energy V gives a function of ρ only which we also denote by V. To calculate the kinetic energy, denoted T_{att}, we allow

$C, G, \boldsymbol{S}$ and ρ in (4.10) to vary with time. We write

$$\hat{R}_i = (\partial_i \hat{U})\hat{U}^\dagger, \qquad \hat{R}_\rho = (\partial_\rho \hat{U})\hat{U}^\dagger \quad \text{and} \quad \boldsymbol{y} = D(G)^{-1}(\boldsymbol{x} - \boldsymbol{S}), \tag{5.1}$$

where ∂_ρ denotes differentiation with respect to ρ; we also introduce the notation $\hat{\boldsymbol{R}}$ for the vector with components $\hat{R}_i$. We then find, in terms of the angular velocities $\boldsymbol{\omega}$ and $\boldsymbol{\Omega}$ defined in section 2,

$$R_0 = C \left([-\tfrac{i}{2}\boldsymbol{\Omega}\cdot\boldsymbol{\tau}, \hat{U}]\hat{U}^\dagger - \boldsymbol{\omega}\cdot\boldsymbol{y} \times \hat{\boldsymbol{R}}_y - \dot{\boldsymbol{S}}\cdot D(G)\hat{\boldsymbol{R}}_y + \dot{\rho}\hat{R}_\rho \right) C^\dagger. \tag{5.2}$$

Here, all functions are evaluated at $\boldsymbol{y}$ and we have written $\hat{\boldsymbol{R}}_y$ to indicate that the differentiation should be carried out with respect to $\boldsymbol{y}$. Inserting this formula into (2.9), changing integration variables to $\boldsymbol{y}$ ($d^3x = d^3y$) and then changing the name of the integration variable from $\boldsymbol{y}$ back to $\boldsymbol{x}$, we find that the kinetic energy can be calculated solely from the standard field $\hat{U}(\rho, \boldsymbol{x})$ and its currents $\hat{R}_i$ and $\hat{R}_\rho$.

The calculation is simplified by symmetries. It follows from the invariance of the kinetic energy T_{att} under the left action of $\mathcal{G}$ that it can be expressed as a (positive, symmetric) bilinear form in $\dot{\rho}$ and the left-invariant angular velocities ω_i and Ω_a ($i, a = 1, 2, 3$). The bilinear form is further restricted by the identifications (4.11) which imply that we should identify the the left-invariant angular velocities $\boldsymbol{\omega}$ and $\boldsymbol{\Omega}$ calculated from $D(C)$ and $D(G)$ with those calculated from the image of $D(C)$ and $D(G)$ under the right action of O_{11}, O_{12} and O_{03}. Explicitly, the angular velocities transform as follows:

$$
\begin{array}{llll}
O_{03} & : (\Omega_1, \Omega_2, \Omega_3) \mapsto (\Omega_1, \Omega_2, \Omega_3) & \text{and} & (\omega_1, \omega_2, \omega_3) \mapsto (-\omega_1, -\omega_2, \omega_3) \\
O_{11} & : (\Omega_1, \Omega_2, \Omega_3) \mapsto (\Omega_1, -\Omega_2, -\Omega_3) & \text{and} & (\omega_1, \omega_2, \omega_3) \mapsto (\omega_1, -\omega_2, -\omega_3) \\
O_{12} & : (\Omega_1, \Omega_2, \Omega_3) \mapsto (\Omega_1, -\Omega_2, -\Omega_3) & \text{and} & (\omega_1, \omega_2, \omega_3) \mapsto (-\omega_1, \omega_2, -\omega_3).
\end{array}
$$

The kinetic energy must respect these identifications, which implies that it is of the following form in the centre of mass frame ($\dot{\boldsymbol{S}} = \boldsymbol{0}$):

$$T_{\text{att}} = \frac{1}{2} \left(f^2 \dot{\rho}^2 + a^2\omega_1^2 + b^2\omega_2^2 + d^2\omega_3^2 + A^2\Omega_1^2 + B^2\Omega_2^2 + C^2\Omega_3^2 + 2e\omega_3\Omega_3 \right), \tag{5.3}$$

where a, b, d, e, f, A, B and C are functions of ρ only. Explicitly we find

$$f^2 = \int d^3x \left\{ -\text{tr}(\hat{R}_\rho \hat{R}_\rho) - \frac{1}{4}\text{tr}([\hat{R}_\rho, \hat{R}_i][\hat{R}_\rho, \hat{R}_i]) \right\}. \tag{5.4}$$

For the spatial moments of inertia we have

$$a^2 = \int d^3x \left\{ -\text{tr}(\boldsymbol{x} \times \hat{\boldsymbol{R}})_1^2 - \frac{1}{4}\text{tr}([(\boldsymbol{x} \times \hat{\boldsymbol{R}})_1, \hat{R}_i][(\boldsymbol{x} \times \hat{\boldsymbol{R}})_1, \hat{R}_i]) \right\} \tag{5.5}$$

and similar formulae for b^2 and d^2 with the free index 1 replaced by 2 and 3 respectively. The moments of inertia in iso-space are given by

$$A^2 = \int d^3x \left\{ \frac{1}{4}\text{tr}([\tau_1, \hat{U}]\hat{U}^\dagger[\tau_1, \hat{U}]\hat{U}^\dagger) + \frac{1}{16}\text{tr}([[\tau_1, \hat{U}]\hat{U}^\dagger, \hat{R}_i][[\tau_1, \hat{U}]\hat{U}^\dagger, \hat{R}_i]) \right\} \tag{5.6}$$

and similar formulae for B^2 and C^2 with τ_1 replaced by τ_2 and τ_3 respectively. Finally the coefficient e of the cross term is

$$e = i \int d^3x \left\{ -\frac{1}{2}\mathrm{tr}([\tau_3, \hat{U}]\hat{U}^\dagger(\boldsymbol{x} \times \hat{\boldsymbol{R}})_3) - \frac{1}{8}\mathrm{tr}([[\tau_3, \hat{U}]\hat{U}^\dagger, \hat{R}_i][(\boldsymbol{x} \times \hat{\boldsymbol{R}})_3, \hat{R}_i]) \right\}. \tag{5.7}$$

In all the above integrals the integrands are invariant under the maps O_{03}, O_{11}, O_{12}. As a result they can be computed by integrating only over the octant $x_i \geq 0$ ($i = 1, 2, 3$) and multiplying the result by 8. Details of how this is done in practice may be found in the appendix.

When $\dot{\boldsymbol{S}} \neq \boldsymbol{0}$ the only additional term in the kinetic energy that is allowed by the requirement of invariance under O_{03}, O_{11} and O_{12} is

$$D(G)_{ik}D(G)_{jl}\dot{S}_i\dot{S}_jM_{kl} \tag{5.8}$$

where the tensor M_{kl} depends on ρ and can be calculated from

$$M_{kl} = \int d^3x \left\{ -\frac{1}{2}\mathrm{tr}(\hat{R}_l\hat{R}_k) - \frac{1}{8}\mathrm{tr}([\hat{R}_l, \hat{R}_n][\hat{R}_k, \hat{R}_n]) \right\}. \tag{5.9}$$

The reflection symmetries of $\hat{R}_i$ imply that M_{lk} is diagonal, so that one needs to calculate three more functions of ρ in order to study the dynamics in an arbitrary inertial frame. In the following we will restrict attention to the centre of mass frame. Thus we will only compute the Lagrangian on the manifold M_7 of centred attractive channel fields.

It is useful to rewrite the expression (5.3) slightly by completing the square:

$$T_{\mathrm{att}} = \frac{1}{2} \left(f^2\dot{\rho}^2 + a^2\omega_1^2 + b^2\omega_2^2 + c^2\omega_3^2 + A^2\Omega_1^2 + B^2\Omega_2^2 + C^2(\Omega_3 + w\omega_3)^2 \right), \tag{5.10}$$

with $c^2 = d^2 - e^2/C^2$ and $w = e/C^2$. The kinetic energy can be expressed in terms of the metric

$$g = f^2d\rho^2 + a^2\sigma_1^2 + b^2\sigma_2^2 + c^2\sigma_3^2 + A^2\Sigma_1^2 + B^2\Sigma_2^2 + C^2(\Sigma_3 + w\sigma_3)^2 \tag{5.11}$$

where σ_i and Σ_a ($i, a = 1, 2, 3$) are the left-invariant one-forms which, when evaluated on a tangent vector to a trajectory in M_7, give the left-invariant angular velocities:

$$\sigma_i(\frac{d}{dt}) = \omega_i \quad \text{and} \quad \Sigma_a(\frac{d}{dt}) = \Omega_a. \tag{5.12}$$

Explicitly, one finds the following formulae in terms of the Euler angles defined earlier

$$\begin{aligned}
\sigma_1 &= \sin\psi d\theta - \cos\psi \sin\theta d\phi \\
\sigma_2 &= \cos\psi d\theta + \sin\psi \sin\theta d\phi \\
\sigma_3 &= d\psi + \cos\theta d\phi,
\end{aligned} \tag{5.13}$$

17

and the corresponding expressions for Σ_a with (ϕ, θ, ψ) replaced by (α, β, γ). One checks that $d\sigma_i = -\frac{1}{2}\epsilon_{ijk}\sigma_j \wedge \sigma_k$ and $d\Sigma_a = -\frac{1}{2}\epsilon_{abc}\Sigma_b \wedge \Sigma_c$. For our discussion we also require the left-invariant vector fields ξ_j on $SO(3)^J$ and ζ_b on $SO(3)^I$ which are dual to the forms σ_i and Σ_a, i.e. $\sigma_i(\xi_j) = \delta_{ij}$ and $\Sigma_a(\zeta_b) = \delta_{ab}$. Explicitly, in terms of Euler angles,

$$
\begin{aligned}
\xi_1 &= \cot\theta \cos\psi \frac{\partial}{\partial\psi} + \sin\psi \frac{\partial}{\partial\theta} - \frac{\cos\psi}{\sin\theta}\frac{\partial}{\partial\phi} \\
\xi_2 &= -\cot\theta \sin\psi \frac{\partial}{\partial\psi} + \cos\psi \frac{\partial}{\partial\theta} + \frac{\sin\psi}{\sin\theta}\frac{\partial}{\partial\phi} \\
\xi_3 &= \frac{\partial}{\partial\psi}.
\end{aligned}
\tag{5.14}
$$

The corresponding formulae for the vector fields ζ_b are obtained by replacing (ϕ, θ, ψ) with (α, β, γ).

For general ρ, the determination of the metric g requires the computation of eight functions of ρ, but when $\rho = \rho_0$ the form of the metric is constrained by the invariance of the field $\hat{U}(\rho_0, \boldsymbol{x})$ under the $SO(2)$ right action (4.8). It follows that we should identify tangent vectors at ρ_0 which are related by the $SO(2)$ right action (4.12). That action can be used to rotate ξ_1 into ξ_2 and ζ_1 into ζ_2. Since the kinetic energy must respect this identification we conclude that, for $\rho = \rho_0$, $g(\xi_1, \xi_1) = g(\xi_2, \xi_2)$ and $g(\zeta_1, \zeta_2) = g(\zeta_2, \zeta_2)$, which implies

$$
a^2(\rho_0) = b^2(\rho_0) \quad \text{and} \quad A^2(\rho_0) = B^2(\rho_0).
\tag{5.15}
$$

Furthermore, the vector field $\xi_3 + 2\zeta_3$ generating the $SO(2)$ action is not defined when $\rho = \rho_0$, and for the metric to be regular there we require that

$$
g(\xi_3 + 2\zeta_3, \xi_3 + 2\zeta_3) = c^2(\rho_0) + C^2(\rho_0)(2 + w(\rho_0))^2 = 0.
\tag{5.16}
$$

Thus, assuming $C(\rho_0) \neq 0$ (equality would imply that ζ_3 also has length zero), it follows that

$$
c(\rho_0) = 0 \qquad \text{and} \qquad w(\rho_0) = -2.
\tag{5.17}
$$

For large ρ, $\hat{U}(\rho, \boldsymbol{x})$ is approximately of the product form, and the potential and kinetic energy can be expressed in terms of the mass and the moment of inertia of the hedgehog field U_H (3.5) and the parameter λ characterising its profile function. Such a calculation was carried out in [15] for the product ansatz constructed from Lorentz-boosted hedgehog solutions. We have repeated that calculation using the instanton-generated hedgehog field for the individual Skyrmions and omitting relativistic corrections. Both of these modifications actually make the calculations harder: in [15] one could exploit the fact that the hedgehog fields in the product ansatz individually satisfy the static equations of motion, and it was found that the relativistic corrections make the final answer simpler than it would otherwise

be. Here we take the centred product ansatz for the attractive channel (3.10) and act with spatial and iso-spatial rotations to obtain

$$CU_H(D(G)^{-1}\boldsymbol{x} + \tfrac{1}{2}R\boldsymbol{e}_1)\tau_3 U_H(D(G)^{-1}\boldsymbol{x} - \tfrac{1}{2}R\boldsymbol{e}_1)\tau_3 C^\dagger. \tag{5.18}$$

Then we insert this field into the Skyrme Lagrangian, allowing the $SU(2)$ matrices C and G and the separation parameter R to vary with time.

The results can be expressed in terms of a single Skyrmion's mass, $M = 147.2$, its moment of inertia, $\Lambda = 140.1$, and its dipole strength, $p = 3.31$. For the potential energy we find the asymptotic formula

$$V \sim 2M - 1.44 \cdot \frac{4\pi p^2}{R^3}, \tag{5.19}$$

and for the moments of inertia

$$
\begin{aligned}
a^2 &\sim 2\Lambda \\
b^2 &\sim \tfrac{1}{2}MR^2 + 2\Lambda - 1.2 \cdot \frac{4\pi p^2}{R} \\
d^2 &\sim \tfrac{1}{2}MR^2 + 2\Lambda - 0.16 \cdot \frac{4\pi p^2}{R} \\
A^2 &\sim 2\Lambda \\
B^2 &\sim 2\Lambda + 2.0 \cdot \frac{4\pi p^2}{R} \\
C^2 &\sim 2\Lambda - 2.0 \cdot \frac{4\pi p^2}{R} \\
e &\sim -2\Lambda + 0.64 \cdot \frac{4\pi p^2}{R},
\end{aligned}
\tag{5.20}
$$

with corrections of order $1/R^2$. It follows that

$$
\begin{aligned}
c^2 &\sim \tfrac{1}{2}MR^2 - 1.04 \cdot \frac{4\pi p^2}{R} \\
w &\sim -1 - 0.68 \cdot \frac{4\pi p^2}{\Lambda R},
\end{aligned}
\tag{5.21}
$$

also with corrections of order $1/R^2$. Apart from the $1/R$ corrections the formulae for the moments of inertia can be understood quite easily in terms of the moments of inertia of the individual Skyrmions and Steiner's theorem. Finally the asymptotic form of the radial metric coefficient is

$$f^2(\rho) \sim \tfrac{1}{2}M + 2.72 \cdot \frac{4\pi p^2}{R^3}. \tag{5.22}$$

As mentioned in section 3, the parameter R can be identified with ρ for large R. Thus the above formulae can be compared with the asymptotic form of the numerically calculated moments of inertia. The agreement is very good for $\rho > 10$. In figures 2 - 6 we plot cubic splines

constructed from our numerical values for the metric coefficients $a^2, b^2, c^2, A^2, B^2, C^2, w$ and f^2; the values for $\rho > 15$ were calculated using the asymptotic expressions (5.20) - (5.22). The numerical values at $\rho = \rho_0$ are $a^2 = 348.5$, $b^2 = 348.4$, $c^2 = 0.0$, $A^2 = B^2 = 229.8$, $C^2 = 130.3$, $w = -2.0$ and $f^2 = 199.9$.

6 Quantisation

Our next goal is to write down the quantum Hamiltonian in the attractive channel and in the centre of mass frame. As a first step we calculate the classical Hamiltonian from the Lagrangian $L_{\text{att}} = T_{\text{att}} - V$ in the usual way. Thus we define the momenta conjugate to the angular velocities $\boldsymbol{\omega}$ and $\boldsymbol{\Omega}$,

$$\boldsymbol{L} = \frac{\partial L_{\text{att}}}{\partial \boldsymbol{\omega}} \qquad \text{and} \qquad \boldsymbol{K} = \frac{\partial L_{\text{att}}}{\partial \boldsymbol{\Omega}}, \tag{6.1}$$

which are the body-fixed angular momenta in space and iso-space. In components,

$$\begin{array}{llll} L_1 = a^2\omega_1, & L_2 = b^2\omega_2, & L_3 = (c^2 + C^2w^2)\omega_3 + wC^2\Omega_3 \\ K_1 = A^2\Omega_1, & K_2 = B^2\Omega_2, & K_3 = C^2(\Omega_3 + w\omega_3). \end{array} \tag{6.2}$$

The corresponding space-fixed spatial angular momentum is $\boldsymbol{J} = D(G)\boldsymbol{L}$ and the space-fixed iso-spatial angular momentum is $\boldsymbol{I} = D(C)\boldsymbol{K}$. Finally defining $P_\rho = \partial L_{\text{att}}/\partial\dot\rho$ we arrive at the classical Hamiltonian in the centre-of-mass frame

$$H_{\text{att}} = \frac{1}{2}\left(\frac{P_\rho^2}{f^2} + \frac{L_1^2}{a^2} + \frac{L_2^2}{b^2} + \frac{(L_3 - wK_3)^2}{c^2} + \frac{K_1^2}{A^2} + \frac{K_2^2}{B^2} + \frac{K_3^2}{C^2}\right) + V(\rho). \tag{6.3}$$

The conserved quantities are the Hamiltonian itself, $\boldsymbol{J}$ and $\boldsymbol{I}$. It follows that $\boldsymbol{L}^2 = \boldsymbol{J}^2$ and $\boldsymbol{K}^2 = \boldsymbol{I}^2$ are also conserved.

In our quantisation scheme the quantum Hamiltonian is

$$H = -\frac{\hbar^2}{2}\Delta + V. \tag{6.4}$$

Here Δ is the covariant Laplace operator associated with the metric g (5.11). Explicitly, in terms of the vector fields ξ_i and ζ_i defined in the previous section,

$$\Delta = \frac{1}{abcABCf}\frac{\partial}{\partial\rho}\left(\frac{abcABC}{f}\frac{\partial}{\partial\rho}\right) + \frac{\xi_1^2}{a^2} + \frac{\xi_2^2}{b^2} + \frac{(\xi_3 - w\zeta_3)^2}{c^2} + \frac{\zeta_1^2}{A^2} + \frac{\zeta_2^2}{B^2} + \frac{\zeta_3^2}{C^2}. \tag{6.5}$$

Physically, $-i\hbar\xi_i$ and $-i\hbar\zeta_i$ are the components of the operators for the angular momenta $\boldsymbol{L}$ and $\boldsymbol{K}$ respectively.

For the rest of this paper we will be concerned with the stationary Schrödinger equation

$$H\Psi = E\Psi. \tag{6.6}$$

The wavefunction Ψ is a section of a (possibly trivial) - complex line bundle over M_7. The structure of the bundle is fixed by Finkelstein-Rubinstein constraints, which we summarise as follows (see also the discussion in [4]). If a single Skyrmion is quantised as a spin $\frac{1}{2}$ particle then the wavefunction for several Skyrmions should pick up a minus sign when one of the Skyrmions is rotated by 2π. Since a rotation of a single Skyrmion by 2π is a non-contractible loop in Q_B for any $B \in \mathbf{Z}$, and since moreover all non-contractible loops are homotopic to this one, wavefunctions are required to be sections of a line bundle over Q_B whose holonomy around any non-contractible loop in Q_B is -1. It follows from the fact that the exchange of two Skyrmions is a non-contractible loop that Skyrmions quantised as half-odd-integer spin particles are fermions and Skyrmions quantised as integer spin particles are bosons. This result, due to Finkelstein and Rubinstein [9], is an example of a topological spin-statistics theorem.

In the section 4 we showed that M_7 has the same zeroth and first homotopy groups as Q_2. Thus, since we quantise a single Skyrmion as a spin $\frac{1}{2}$ particle, Ψ should be a section of a non-trivial bundle over M_7 such that its holonomy around a non-contractible loop in M_7 is -1. It is sufficient to impose this for one such loop, and we will use the loop Γ_{11}, which, for well-separated Skyrmions, is the rotation of one Skyrmion by 2π. The simplest way to implement the Finkelstein-Rubinstein constraints is to think of Ψ as a function on the double cover $\tilde{M}_7$ of M_7 and to impose the equivariance condition

$$\Psi \circ O_{11} = -\Psi. \tag{6.7}$$

Points related by O_{03} are still identified in $\tilde{M}_7$, so Ψ must obey

$$\Psi \circ O_{03} = \Psi. \tag{6.8}$$

Then, since $O_{12} = O_{11}O_{03}$ it follows that

$$\Psi \circ O_{12} = -\Psi. \tag{6.9}$$

In accordance with our interpretation of O_{12} this last condition shows that the two Skyrmions are fermions, *i.e.* that the wavefunction is odd under their exchange. The important point here is that M_7 captures enough of the topology of Q_2 for the topological spin-statistics theorem to hold.

Exploiting the symmetry of the Hamiltonian we separate variables by introducing Wigner functions $D^j_{sm}(\phi, \theta, \psi)$ and $D^i_{tn}(\alpha, \beta, \gamma)$ on $SO(3)^J$ and $SO(3)^I$ respectively, following the conventions of [16]. The former are simultaneous eigenfunctions of the square of the total spin operator $\boldsymbol{L}^2 = \boldsymbol{J}^2 = -\hbar^2(\xi_1^2 + \xi_2^2 + \xi_3^2)$, the third component of the space-fixed spin operator $J_3 = -i\hbar\partial/\partial\phi$ and the third component of the body-fixed spin operator $L_3 = -i\hbar\partial/\partial\psi$:

$$\boldsymbol{L}^2 D^j_{sm} = j(j+1)\hbar^2 D^j_{sm}, \qquad J_3 D^j_{sm} = m\hbar D^j_{sm}, \qquad L_3 D^j_{sm} = s\hbar D^j_{sm}. \tag{6.10}$$

Similarly, $D_{tn}^i(\alpha, \beta, \gamma)$ is an eigenfunction of the square of the total iso-spin operator $\boldsymbol{K}^2 = \boldsymbol{I}^2 = -\hbar^2(\zeta_1^2 + \zeta_2^2 + \zeta_3^2)$, the third component of the space-fixed iso-spin operator $I_3 = -i\hbar\partial/\partial\alpha$ and the third component of the body-fixed iso-spin operator $K_3 = -i\hbar\partial/\partial\gamma$:

$$\boldsymbol{K}^2 D_{tn}^i = i(i+1)\hbar D_{tn}^i, \qquad I_3 D_{tn}^i = n\hbar D_{tn}^i, \qquad K_3 D_{tn}^i = t\hbar D_{tn}^i. \tag{6.11}$$

The Wigner functions are normalised so that

$$\int |D_{sm}^j|^2 \sin\theta \, d\phi \, d\psi \, d\theta = \frac{8\pi^2}{2j+1} \qquad \text{and} \qquad \int |D_{tn}^i|^2 \sin\beta \, d\alpha \, d\gamma \, d\beta = \frac{8\pi^2}{2i+1}. \tag{6.12}$$

Since both spatial and iso-spatial rotations by 2π are contractible in M_7 we must use Wigner functions which are even under such rotations and hence i and j are positive integers and n, t, m, s are integers in the ranges $-i \leq n, t \leq i$ and $-j \leq m, s \leq j$. Wigner functions of integer spin transform under the discrete maps (6.8) and (6.7) as follows

$$\begin{aligned} D_{sm}^j \circ O_{03} &= (-1)^s D_{sm}^j \\ D_{tn}^i D_{sm}^j \circ O_{11} &= (-1)^{i+j} D_{-t,n}^i D_{-s,m}^j. \end{aligned} \tag{6.13}$$

When looking for bound states of the Schrödinger equation (6.6) we can fix the quantum numbers j (total spin), i (total iso-spin), m (the third component of the space-fixed spin) and n (the third component of the space-fixed iso-spin). We are interested in two nucleon bound states, so $i = 0$ or $i = 1$. The Wigner function for $i = j = 0$ (which is constant) does not satisfy (6.13). For the quantum numbers of the deuteron, $(i, j) = (0, 1)$, there is exactly one state (we do not count Wigner functions differing in m or n as different states), which we write as

$$\Psi = \sqrt{\frac{3}{8\pi^2}} D_{0m}^1(\phi, \theta, \psi) u(\rho). \tag{6.14}$$

Inserting Ψ into (6.6) we obtain the following differential equation for u:

$$\frac{1}{abcABCf}\frac{d}{d\rho}\left(\frac{abcABC}{f}\frac{du}{d\rho}\right) + \left(\frac{2}{\hbar^2}(E-V) - \frac{1}{a^2} - \frac{1}{b^2}\right)u = 0. \tag{6.15}$$

For $(i, j) = (1, 0)$, the iso-vector states, there are two allowed angular states. The ansatz

$$\Psi = \sqrt{\frac{3}{8\pi^2}} D_{0n}^1(\alpha, \beta, \gamma) u(\rho) \tag{6.16}$$

leads to the differential equation

$$\frac{1}{abcABCf}\frac{d}{d\rho}\left(\frac{abcABC}{f}\frac{du}{d\rho}\right) + \left(\frac{2}{\hbar^2}(E-V) - \frac{1}{A^2} - \frac{1}{B^2}\right)u = 0. \tag{6.17}$$

The second possibility is

$$\Psi = \sqrt{\frac{3}{16\pi^2}}(D^1_{1n} + D^1_{-1,n})(\alpha, \beta, \gamma)u(\rho) \tag{6.18}$$

and leads to

$$\frac{1}{abcABCf}\frac{d}{d\rho}\left(\frac{abcABC}{f}\frac{du}{d\rho}\right) + \left(\frac{2}{\hbar^2}(E - V) - \frac{1}{A^2} - \frac{w^2}{c^2} - \frac{1}{C^2}\right)u = 0. \tag{6.19}$$

To study more general bound states and scattering solutions of (6.6) one can use techniques similar to the ones used in [18] to study the quantum dynamics of two magnetic monopoles in the moduli space approximation. One should make the ansatz

$$\Psi(\phi, \theta, \psi, \alpha, \beta, \gamma, \rho) = \sum_{jsmitn} D^i_{tn}(\alpha, \beta, \gamma)D^j_{sm}(\phi, \theta, \psi)u^{ij}_{tn,sm}(\rho), \tag{6.20}$$

where the sum runs over the indices of the Wigner functions, suitably restricted by conservation laws and the constraints (6.7) - (6.9). For bound states, one may fix i, j, n and m, and one will typically need to solve a set of coupled ordinary differential equations for the functions $u^{ij}_{tn,sm}(\rho)$, $-i \leq t \leq i$, $-j \leq s \leq j$. To obtain scattering solutions one necessarily needs to consider an infinite sum over j, and in principle one needs to solve infinitely many systems of coupled ordinary differential equations. However, to compute scattering cross sections at low energy it is sufficient to study the systems of equations that arise for small j.

In this paper we will only study bound state problems and restrict attention to the uncoupled ordinary differential equations (6.15), (6.17) and (6.19).

7 Quantum Bound States

To find the lowest eigenvalue of the deuteron equation (6.15) we need approximate analytic solutions near $\rho = \rho_0$ and for large ρ. To find these it is useful to define the effective potential

$$V_{\text{eff}} = V - 2M + \frac{\hbar^2}{2}\left(\frac{1}{a^2} + \frac{1}{b^2} - \frac{1}{2\Lambda}\right), \tag{7.1}$$

which tends to zero as $\rho \to \infty$. In figure 7 we plot both the classical potential $V - 2M$ and the effective potential V_{eff}. Also defining the shifted energy

$$\varepsilon = E - 2M - \frac{\hbar^2}{4\Lambda}, \tag{7.2}$$

equation (6.15) becomes

$$\frac{1}{abcABCf}\frac{d}{d\rho}\left(\frac{abcABC}{f}\frac{du}{d\rho}\right) + \frac{2}{\hbar^2}(\varepsilon - V_{\text{eff}})u = 0. \tag{7.3}$$

For ρ near ρ_0, we define $h = \rho - \rho_0$, and the equation becomes approximately the Bessel equation

$$\frac{1}{h}\frac{d}{dh}\left(h\frac{du}{dh}\right) + \frac{2f^2(\rho_0)}{\hbar^2}\left(\varepsilon - V_{\text{eff}}(\rho_0)\right)u = 0, \tag{7.4}$$

which has only one solution that is regular at the origin, namely the Bessel function J_0 of zeroth order. Thus, for small h

$$u(\rho_0 + h) \propto J_0\left(\sqrt{\frac{2f^2(\rho_0)}{\hbar^2}\left(\varepsilon - V_{\text{eff}}(\rho_0)\right)}h\right). \tag{7.5}$$

It follows in particular that u is non-zero at ρ_0 and that it has vanishing derivative there.

For large ρ the equation (7.3) becomes

$$\frac{1}{\rho}\frac{d^2(\rho u)}{d\rho^2} + \frac{M\varepsilon}{\hbar^2}u = 0, \tag{7.6}$$

which has two solutions, one exponentially growing and one exponentially decaying. A normalisable wavefunction has to be asymptotically proportional to the latter:

$$u \propto \frac{e^{-\frac{\sqrt{-M\varepsilon}}{\hbar}\rho}}{\rho}. \tag{7.7}$$

Imposing the behaviour (7.5) and (7.7) near ρ_0 and for large ρ we have numerically searched for normalisable eigenfunctions of (7.3), using a shooting method; we find that there is precisely one, which we denote by u_d and which we normalise so that

$$\int_{\rho_0}^{\infty} d\rho\, u_d^2 abcABCf = 1. \tag{7.8}$$

The corresponding eigenvalue is $\varepsilon_d = -1.107$ in geometrical units, or $\varepsilon_d = -6.18$ MeV in physical units. We also note that the corresponding eigenvalue of the original Schrödinger equation (6.6) is, according to (7.2), $E_d = 2M + \hbar^2/4\Lambda + \varepsilon_d = 1658.4$ MeV in physical units. In the following, the wavefunction (6.14) with u_d for u and $m = 1$ ('spin up'), namely

$$\Psi_d = \sqrt{\frac{3}{8\pi^2}}D_{01}^1(\phi, \theta, \psi)u_d(\rho) = -\sqrt{\frac{3}{16\pi^2}}\sin\theta e^{i\phi}u_d(\rho) \tag{7.9}$$

will be referred to as the deuteron wavefunction. In figures 8.a) and 8.b) we show plots of u_d and of the normalised probability density $u_d^2(\rho)abcABCf$.

The translation of the eigenvalue ε_d of (7.3) into a theoretical prediction for the deuteron binding energy requires some thought. Physically, the deuteron's binding energy is defined as the energy required to break a deuteron up into two infinitely separated nucleons, one proton and one neutron. However, in this paper we are only considering two-Skyrmions in the attractive channel, and therefore wavefunctions on M_7, the space of attractive channel fields,

24

can only describe two nucleons with correlated spin and iso-spin. Thus, while the energy of two free nucleons is $2M + 3\hbar^2/4\Lambda = 1708.2$ MeV, the eigenvalue ε_d measures the binding relative to the energy of infinitely separated two nucleons in the attractive channel and with total iso-spin and spin quantum numbers $(i, j) = (0, 1)$, which is $2M + \hbar^2/4\Lambda$ or 1664.6 MeV. However, it would be naive to simply add the difference of $-\hbar^2/2\Lambda = -43.6$MeV to ε_d and interpret the result as the true binding energy of the deuteron. Rather, a precise calculation of the deuteron's binding energy would require solving the Schrödinger equation on the full twelve-dimensional moduli space M_{12} discussed in the introduction. That is a difficult task, but it may be possible to take into account the extra degrees of freedom approximately by treating them as small oscillations around the attractive channel fields. Then one might be able to estimate the effect of the extra degrees of freedom on the Schrödinger equation for the deuteron by including their zero point energies in the effective potential V_{eff}. These zero point energies depend on ρ, but in a first, crude approximation one may describe the net effect by adding a constant to V_{eff}. From the above discussion of well-separated nucleons in our model we know that the constant should be approximately 43.6 MeV. It then follows that the binding energy of -6.18 MeV, which we calculated by restricting attention to attractive channel fields, is also an estimate of the binding energy calculated in a more careful treatment involving the larger manifold of collective coordinates M_{12}.

It is interesting to convert the quantum mechanical probability distribution $|\Psi|^2(\rho, \phi, \theta, \psi)$ of a quantum state Ψ on the moduli space into a probability distribution $p_\Psi(\boldsymbol{x})$ on physical space in such a way that $p_\Psi(\boldsymbol{x})d^3x$ can be interpreted as the probability of finding one of the nucleons in the region $[x_1, x_1 + dx_1] \times [x_2, x_2 + dx_2] \times [x_3, x_3 + dx_3]$. Strictly speaking such a translation only makes sense for Skyrme fields consisting of two well-separated Skyrmions. For such fields the baryon number density B^0 is peaked near the individual Skyrmions' positions and may be interpreted as the 'particle density' of the Skyrme field. When the Skyrmions coalesce it is no longer meaningful to talk about the individual Skyrmions, but one can still interpret the baryon number density as the 'density of Skyrme matter'. To find the probability distribution $p_\Psi(\boldsymbol{x})$ of Skyrme matter for a given quantum state Ψ on the moduli space, one should average the classical baryon number density over the moduli space, weighted by $|\Psi|^2$. Thus, writing $\hat{B}^0(\rho, \boldsymbol{x})$ for the baryon number density (2.12) of an attractive channel field in the standard orientation and with separation parameter ρ, we define the spatial probability distribution $p_d(\boldsymbol{x})$ for the deuteron state as

$$p_d(\boldsymbol{x}) = \frac{1}{2} \int \hat{B}^0(\rho, D(G)^{-1}\boldsymbol{x})|\Psi_d|^2 \sin\theta \, abcABCf \, d\rho \, d\theta \, d\phi \, d\psi \,. \tag{7.10}$$

Here the $SO(3)$ matrix $D(G)$ is parametrised in terms of the Euler angles (ϕ, θ, ψ) according to (4.13). To evaluate this expression we introduce spherical coordinates (r, Θ, Φ) for $\boldsymbol{x}$, so that $\boldsymbol{x} = r(\sin\Theta\cos\Phi, \sin\Theta\sin\Phi, \cos\Theta)$ and a further set of spherical coordinates $(r, \tilde{\theta}, \tilde{\phi})$ for $\tilde{\boldsymbol{x}} = D(G)^{-1}\boldsymbol{x}$, i.e. $\tilde{\boldsymbol{x}} = r(\sin\tilde{\theta}\cos\tilde{\phi}, \sin\tilde{\theta}\sin\tilde{\phi}, \cos\tilde{\theta})$. Then, by expanding $\hat{B}^0(\rho, \tilde{\boldsymbol{x}})$ for

fixed ρ and r in spherical harmonics $Y_{lm}(\tilde{\theta}, \tilde{\phi})$, and by using the transformation properties of spherical harmonics under rotations, one shows that p_d depends only on r and Θ, and that it is given by

$$
\begin{aligned}
p_d(r, \Theta) \;=\; & \frac{1}{8\pi} \int \hat{B}^0(\rho, \tilde{\boldsymbol{x}}) u_d^2(\rho)\, abc\, ABCf\, \sin\tilde{\theta}\, d\rho\, d\tilde{\theta}\, d\tilde{\phi} \\
& - \frac{1}{32\pi}(1 - 3\cos^2\Theta) \int \hat{B}^0(\rho, \tilde{\boldsymbol{x}}) u_d^2(\rho)(1 - 3\cos^2\tilde{\theta})\, abc\, ABCf\, \sin\tilde{\theta}\, d\rho\, d\tilde{\theta}\, d\tilde{\phi}.
\end{aligned}
\tag{7.11}
$$

In the conventional description of the deuteron as a bound state of two point-like nucleons, the square of the modulus of the deuteron wavefunction also gives the probability of finding one of the nucleons in a given region of space. It is therefore meaningful to compare $p_d(r, \Theta)$ with such a probability distribution calculated in a conventional model. That comparison is made in figure 9. The distributions are clearly very similar. Thus, although the classical toroidal bound state of two Skyrmions looks radically different from the conventional picture of the deuteron (a point often raised as a criticism of the Skyrme model) the two approaches lead to remarkably similar spatial probability distributions of nuclear matter at the quantum level.

To study the quantum states with $(i, j) = (1, 0)$ we need to consider the two radial equations (6.17) and (6.19). There is no bound state solution of (6.19), essentially because c^2 vanishes at ρ_0, giving rise to a strongly repulsive centrifugal potential w^2/c^2. The equation (6.17), however, does have a bound state solution. It can be brought into the same form as the deuteron equation (7.3), but now the shifted energy ε is

$$
\varepsilon = E - 2M - \frac{\hbar^2}{2\Lambda}
\tag{7.12}
$$

and the effective potential is

$$
V_{\text{eff}} = V - 2M + \frac{\hbar^2}{2}\left(\frac{1}{A^2} + \frac{1}{B^2} - \frac{1}{\Lambda} \right),
\tag{7.13}
$$

which tends to zero as $\rho \to \infty$. There is a unique bound state solution which, like the deuteron wavefunction, is non-vanishing at ρ_0 and has zero derivative there. We will not go into the details here, but simply note the numerical value of the bound state energy, which is $\varepsilon_{NN} = -1.74$ in geometrical units, or $\varepsilon_{NN} = -9.74$ MeV in physical units. It follows that $E_{NN} = 1676.7$ MeV.

In nature, the deuteron is the only bound state of two nucleons. However, there is a marginally unbound state with quantum numbers $(i, j) = (1, 0)$, the iso-vector $^1S_0$ state. In our model this state is the one with energy E_{NN}. Our model gives the right ordering of energy levels $E_d < E_{NN}$, and an energy difference $E_{NN} - E_d$ of the right order of magnitude.

Moreover, $E_{NN} + 43.6$ MeV > 1708.2 MeV, the energy of two free nucleons. Thus if, as argued above, the effect of including the two extra degrees of freedom is to push the energy levels up by 43.6 MeV, then the $(i, j) = (1, 0)$ bound state we found here will not persist when all 12 degrees of freedom of M_{12} are taken into account.

8 Electrostatic Properties of the Deuteron

The first attempt to calculate the Skyrme model's predictions for the deuteron's electrostatic properties was made by Braaten and Carson in [4] under the assumption that the deuteron can be described as a quantum state of a toroidal Skyrmion. We will briefly review and then use their basic formulae for the classical electrostatic properties of a Skyrme field. Since we are using a larger number of collective coordinates than in [4], our calculation of quantum mechanical expectation values will, however, be different.

The starting point of the calculations is the basic relationship, first derived in [17], between the electromagnetic current j_μ, the third component of the (classical) iso-spin current I_μ^3 and the baryon number current B_μ introduced in (2.11):

$$j_\mu = \tfrac{1}{2}B_\mu + I_\mu^3. \tag{8.1}$$

We are only interested in the expectation values of various classical multipole tensors for quantum states with zero iso-spin, so we set I_μ^3 to zero in the following and replace j_μ by $\tfrac{1}{2}B_\mu$. It is sufficient to perform the computations of the various tensors with the Skyrme fields in their standard orientation. Specifically, we will compute the theoretical predictions for the deuteron's electric charge radius, its electric quadrupole moment and its magnetic dipole moment. We will first discuss the general formulae for these quantities and then compile the numerical results in a table.

First consider the root mean square (rms) electric charge radius of an attractive channel field. It is a function of ρ only and defined as the square root of

$$r_{\mathrm{rms}}^2(\rho) = \tfrac{1}{2} \int d^3x |\boldsymbol{x}|^2 B^0(\rho, \boldsymbol{x}). \tag{8.2}$$

The theoretical prediction for the deuteron's rms electric charge radius r_c is the square root of

$$r_c^2 = \langle \Psi_d | r_{\mathrm{rms}}^2 | \Psi_d \rangle = \int_{\rho_0}^{\infty} d\rho\, r_{\mathrm{rms}}^2 u_d^2 abcABCf. \tag{8.3}$$

Next, the classical electric quadrupole tensor for an attractive channel field in standard orientation also depends only on ρ and is given by

$$\hat{Q}_{ij}(\rho) = \tfrac{1}{2} \int d^3x (3x_i x_j - |\boldsymbol{x}|^2 \delta_{ij}) \hat{B}^0(\rho, \boldsymbol{x}). \tag{8.4}$$

It follows from the discrete symmetries of the attractive channel fields that $\hat{Q}_{ij}$ is diagonal. It is also traceless, so it contains only 2 independent components ($\hat{Q}_{11}$ and $\hat{Q}_{22}$, say). Moreover, at ρ_0, $\hat{Q}_{11} = \hat{Q}_{22}$. The quadrupole tensor for a field in general orientation G is given by

$$Q_{lm} = D(G)_{li}D(G)_{mj}\hat{Q}_{ij} \tag{8.5}$$

and the deuteron's quadrupole moment is defined as

$$Q = \langle \Psi_d | Q_{33} | \Psi_d \rangle. \tag{8.6}$$

Performing the angular integration one finds

$$Q = \tfrac{1}{5} \int_{\rho_0}^{\infty} d\rho \, (\hat{Q}_{11} + \hat{Q}_{22}) u_d^2 abcABCf. \tag{8.7}$$

Finally, the iso-scalar ($I_\mu^3 = 0$) part of the magnetic dipole moment is defined as

$$\mu_i(\rho) = \tfrac{1}{4} \int \epsilon_{ijk} x_j B_k(\rho, \boldsymbol{x}) d^3 x. \tag{8.8}$$

For fields in the standard orientation it can be written

$$\hat{\mu}_i = \hat{M}_{ia}\Omega_a + \hat{m}_{ik}\omega_k, \tag{8.9}$$

where

$$
\begin{aligned}
\hat{M}_{ia} &= \frac{1}{32\pi^2} \int d^3 x \, x_j \text{tr}([\hat{R}_i, \hat{R}_j][-\frac{i}{2}\tau_a, \hat{U}]\hat{U}^\dagger) \\
\hat{m}_{ik} &= -\frac{1}{32\pi^2} \int d^3 x \, \epsilon_{kmn} x_j x_m \text{tr}([\hat{R}_i, \hat{R}_j]\hat{R}_n).
\end{aligned} \tag{8.10}
$$

It follows from the discrete symmetries of the attractive channel fields that both $\hat{M}_{ia}$ and $\hat{m}_{il}$ are symmetric, and that the only non-zero component of $\hat{M}_{ia}$ is $\hat{M}_{33}$. In fact, we shall see shortly that we only need $\hat{m}_{11}$ and $\hat{m}_{22}$ when computing the deuteron's magnetic dipole moment. Explicitly one finds

$$
\begin{aligned}
\hat{m}_{11}(\rho) &= \tfrac{1}{4} \int d^3 x (x_2^2 + x_3^2) \hat{B}^0(\rho, \boldsymbol{x}) \\
\hat{m}_{22}(\rho) &= \tfrac{1}{4} \int d^3 x (x_1^2 + x_2^2) \hat{B}^0(\rho, \boldsymbol{x});
\end{aligned} \tag{8.11}
$$

at ρ_0 these two quantities are equal. To compute the deuteron's magnetic moment, defined via

$$\mu = \langle \Psi_d | \mu_3 | \Psi_d \rangle, \tag{8.12}$$

we require the magnetic moments of the attractive channel fields in arbitrary orientation G, which are given by

$$\mu_l(\rho) = D(G)_{li}\hat{\mu}_i(\rho). \tag{8.13}$$

Then, in order to calculate the expectation value in the quantum state of the deuteron, we should replace ω_1, ω_2 and ω_3 by the operators $L_1/a^2, L_2/b^2$ and L_3/c^2, and similarly Ω_1, Ω_2 and Ω_3 by the operators $K_1/A^2, K_2/B^2$ and K_3/C^2. Since the components of the body-fixed angular momentum operator $\boldsymbol{L}$ do not commute with the entries of the matrix $D(G)$ there is potentially an operator ordering ambiguity in evaluating matrix elements of the operator μ_l, but in the calculation of the expectation value in the deuteron state this ambiguity does not arise. Here we find

$$\mu = \frac{\hbar}{2} \int_{\rho_0}^{\infty} d\rho \, (\frac{\hat{m}_{11}}{a^2} + \frac{\hat{m}_{22}}{b^2})u_d^2 abcABCf. \tag{8.14}$$

In nature, the magnetic dipole moment of the deuteron is almost exactly equal to the sum of the magnetic dipole moments μ_p and μ_n of the proton and the neutron. In conventional models of the deuteron as a bound state of a proton and neutron the discrepancy can be related to the d-wave contribution in the deuteron wavefunction [19]. It is instructive for us to carry out a similar comparison, but here we should compare our result for the deuteron's magnetic dipole moment with the sum of the proton's and neutron's magnetic dipole moments as calculated in the Skyrme model with the appropriate parameters.

We list our numerical results in the table below. We have followed the practice in nuclear physics of measuring magnetic dipole moments in units of the nuclear magneton (nm) $\hbar/2M_N$, where $M_N = 939$ MeV is the physical nucleon mass. For comparison we also list the results obtained by Braaten and Carson in their treatment of the deuteron as a toroidal Skyrmion. The experimental values are taken from [20]. In the first row we compare values for the deuteron binding energy. Under Braaten & Carson we quote the value which Braaten and Carson calculated in [4] by computing the difference between the energy of their deuteron state and the energy of two free nucleons. Braaten and Carson did not in fact attach much meaning to this particular result of their calculations and pointed out that one should take into account vibrational modes of the toroidal configurations for a meaningful calculation of the deuteron's binding energy. The comparison in our table shows that the inclusion of the softest vibrational mode alone - the deformation of a toroidal configuration within the attractive channel manifold M_{10} - reduces the prediction for the binding energy by an order of magnitude, and brings it close to the experimental value. In the last row, the theoretical predictions for μ_p and μ_n are calculated in the Skyrme model using the formulae given by Adkins *et al.* in [6]. These formulae depend on the profile function for the hedgehog field with unit baryon number and on the choice of the constants F_π and e. For the latter we use the values assumed throughout this paper and given in (2.5). Then, to calculate the value of $\mu_p + \mu_n$ in our model we use the instanton generated profile function (3.6); the value listed under Braaten & Carson is taken from the analysis of Adkins and Nappi in [7] which is based on the same values for F_π, e and the pion mass as used by Braaten and Carson.

	Theory		Experiment
	this model	Braaten & Carson	
ε_d [MeV]	-6.18	-158	-2.225
r_c [fermi]	2.18	0.92	2.095
Q [fermi²]	0.83	0.082	0.2859
μ [nm]	0.55	0.74	0.8574
$\mu_p + \mu_n$ [nm]	0.41	0.55 (from [7])	0.8797

Table 1

Deuteron Properties

9   Discussion

In this paper we have described the deuteron as a quantum state of instanton-generated two-Skyrmions in the attractive channel. This picture seems qualitatively correct and leads to predictions for certain deuteron observables which are also in reasonable quantitative agreement with experiment. However, our calculations clearly involve a number of approximations, and from the point of view of the general approach to two-Skyrmion dynamics outlined in the introduction, two of these deserve a more careful discussion. Firstly, we obtained our Skyrme fields by computing instanton holonomies and not, as suggested in the introduction, by calculating paths of steepest descent in the Skyrme model. This means in particular that we cannot take into account the physical pion mass. The experience with the static properties of a single nucleon in the Skyrme model shows that the inclusion of the pion mass does not affect the results very much. We expect similarly that the plots 2 - 6 and 7 of the metric coefficients and the potential would not be qualitatively different for fields calculated via paths of steepest descent in the Skyrme model with a pion mass term. There is one obvious difference which would occur in the asymptotic form of the plots: while the

potential and metric coefficients calculated above approach their asymptotic values according to a power law, the approach would be exponentially fast in a model with non-zero pion mass. This difference would be important if one were to discuss nucleon-nucleon scattering. However, it does not matter much for the calculations presented above because the deuteron wavefunction is not very sensitive to the asymptotic form of the Hamiltonian.

The other, more serious simplification we made was to consider the ten-dimensional moduli space M_{10} instead of the twelve-dimensional space M_{12} described in the introduction. The validity of this approximation is much harder to assess, but the following comments may elucidate its physical meaning. It has been known for a long time (see e.g. [22]) that, for zero pion mass, the potential energy for the interaction of two well-separated Skyrmions with arbitrary individual positions and orientations is, up to a positive constant of proportionality,

$$- (1 - \cos\chi)\frac{1 - 3(\boldsymbol{n}\cdot\hat{\boldsymbol{R}})^2}{R^3}, \tag{9.1}$$

where $\boldsymbol{R}$ is the relative position vector, $\hat{\boldsymbol{R}} = \boldsymbol{R}/R$ and $(\boldsymbol{n}, \chi)$ are the axis and rotation angle for the $SO(3)$ matrix describing the relative orientation. In the attractive channel, the relative orientation is chosen so as to minimise the potential energy at fixed R. Thus, χ is set to π and $\boldsymbol{n}$ is required to be orthogonal to $\hat{\boldsymbol{R}}$. This eliminates two degrees of freedom, but it still allows for rotations of $\boldsymbol{n}$ in the plane orthogonal to $\hat{\boldsymbol{R}}$.

The potential (9.1) is the classical analogue, in the Skyrme model, of the one pion exchange tensor potential in conventional nuclear physics [22]. To calculate nuclear forces from it one should compute its expectation value in states which are tensor products of the free nucleon wave functions given in [6]. In particular, the expectation value of (9.1) in the triplet state with total spin 1 and total isospin 0 (the quantum numbers of the deuteron) is a 3×3 matrix which can be expressed in terms of the total spin operator $\boldsymbol{s}$. It is, up to an overall positive constant of proportionality

$$V_{\mathrm{T}} = \frac{2 - 3(\boldsymbol{s}\cdot\hat{\boldsymbol{R}})^2}{R^3}. \tag{9.2}$$

At fixed R, this expression is minimal when the total spin is parallel to the separation vector $\boldsymbol{R}$. The assumption of the attractive channel approximation is that the relative orientation is always such that the potential is minimal at given R. Thus, working with attractive channel fields amounts, in the language of nuclear physics, to assuming that the total nucleon spin is always aligned with the relative separation vector or, equivalently, that the torque resulting from the tensor force is infinitely strong.

In conventional discussions of the deuteron and its properties the tensor force is responsible for the existence of a d-wave contribution to the deuteron wavefunction The d-wave probability in turn is linked to physical observables. In the absence of a d-wave the deuteron's

electric quadrupole moment would be zero and the deuteron's magnetic dipole moment would equal the sum of the proton's and the neutron's magnetic dipole moments. Both the size of the quadrupole moment Q and the difference $\mu - (\mu_p + \mu_n)$ are therefore direct measures of the d-wave probability, which in turn indicates the strength of the tensor potential. Thus, since the truncation of M_{12} to the space of attractive channel fields systematically overestimates the strength of the tensor force, it is not surprising that our theoretical predictions for Q and $\mu - (\mu_p + \mu_n)$ are rather large. Quantising the extra two degrees of freedom included in M_{12}, at least approximately, may well bring the predictions much closer to the experimental values.

A   Numerical Methods

In this appendix we give a detailed and in parts technical account of our method for computing the potential V in the attractive channel, the metric g derived from the kinetic energy T_{att}, and the quantities required in the calculation of static deuteron properties. All these depend only on the Skyrmion separation ρ, and in equations (2.10), (5.4)-(5.7) and (8.2)-(8.11) we have shown how to write them as integrals over physical space of various combinations of the Skyrme fields $\hat{U}(\rho, \boldsymbol{x})$ and their currents. The metric g has eight non-vanishing components, and it turns out that the deuteron's static properties can be expressed in terms of three independent moments of the baryon number density $\hat{B}^0$. Including the potential, there are thus twelve functions of ρ to be computed.

The computational method is similar to that used in [23] to find classical bound states of three and four Skyrmions, although several additions and refinements are necessary to carry the programme through successfully. The following paragraphs concentrate on these new

features; [23] should be consulted for the remaining details. There are two tasks: firstly the solution of the holonomy equation (3.2) to construct the attractive channel Skyrme fields in standard orientation, and then integrations over all space to obtain the required functions of ρ.

Recall that the attractive channel Skyrme fields are obtained from instantons which depend on two essential parameters. In the standard orientation, for which the relevant Hartshorne data is depicted in figure 1, these may be taken to be the scale L and the angle ϑ. Thus, the solutions of the holonomy equation (3.2) for these instantons are Skyrme fields on $\mathbf{R}^3$ which also depend on L and ϑ; we denote them by $\hat{U}(L, \vartheta, \boldsymbol{x})$. It follows from the definition of $\hat{U}(L, \vartheta, \boldsymbol{x})$ and from the scaling behaviour of JNR instantons that

$$\hat{U}(L, \vartheta, \boldsymbol{x}) = \hat{U}(1, \vartheta, \frac{\boldsymbol{x}}{L}). \tag{A.1}$$

Hence the current $\hat{\boldsymbol{R}}_i(L, \vartheta, \boldsymbol{x}) = (\partial_i \hat{U}(L, \vartheta, \boldsymbol{x})) U^\dagger(L, \vartheta, \boldsymbol{x})$ satisfies

$$\hat{\boldsymbol{R}}_i(L, \vartheta, \boldsymbol{x}) = \frac{1}{L} \hat{\boldsymbol{R}}_i^L(1, \vartheta, \frac{\boldsymbol{x}}{L}), \tag{A.2}$$

where on the right-hand side the superscript L indicates that the differentiation should be carried out with respect to $\boldsymbol{x}/L$. To obtain the Skyrme fields $\hat{U}(\rho, \boldsymbol{x})$ used in the main body of the paper, the scale L is fixed for each value of ϑ at the value $L(\vartheta)$ which minimises the potential energy (2.10). Explicitly, writing E_2 and E_4 for the quadratic and the quartic terms in the potential energy (2.10) evaluated on the field $\hat{U}(1, \vartheta, \boldsymbol{x})$, this is

$$L(\vartheta) = \sqrt{\frac{E_4}{E_2}}. \tag{A.3}$$

In practice, it is most convenient to compute all fields and currents at the scale $L = 1$ and to find the fields and currents at the relevant scale $L(\vartheta)$ using the formulae (A.1) and (A.2).

It remains to explain the computation of the current $\hat{\boldsymbol{R}}_\rho$ (5.1), which requires some care. After fixing the scale at $L(\vartheta)$ the formula $\rho = 2L(\vartheta)(1 - \sin\vartheta)$ establishes a one-to-one relation between ρ and ϑ. Thus, both ϑ and L may be thought of as functions of ρ, and we can write

$$\partial_\rho \hat{U}(L, \vartheta, \boldsymbol{x}) = \left(\frac{dL}{d\rho}\right)\partial_L \hat{U}(L, \vartheta, \boldsymbol{x}) + \left(\frac{d\vartheta}{d\rho}\right)\partial_\vartheta \hat{U}(L, \vartheta, \boldsymbol{x}). \tag{A.4}$$

Using the relation (A.1), the derivative of $\hat{U}$ with respect to L may be expressed in terms of the currents $\hat{R}_i$:

$$\partial_L \hat{U}(L, \vartheta, \boldsymbol{x}) \hat{U}^\dagger(L, \vartheta, \boldsymbol{x}) = -\sum_i \left(\frac{x_i}{L}\right) \hat{R}_i(L, \vartheta, \boldsymbol{x}). \tag{A.5}$$

Thus it is the derivative of $\hat{U}$ with respect to ϑ, or equivalently the current $\hat{R}_\vartheta = (\partial_\vartheta \hat{U})\hat{U}^\dagger$, that has to be calculated directly from the holonomy equations. Finally, the linear combination on the right-hand side of (A.4) is computed after the scaling factors $L(\vartheta)$ have been

calculated; $dL/d\rho$ and $d\vartheta/d\rho$ may then be found efficiently by fitting a cubic spline to the values of L at each ϑ.

For further details of the numerical integration of the holonomy equation (3.2) we refer the reader to [23]. In particular it is explained there how the currents $\hat{R}_i$ can be found directly from a holonomy equation involving the differentiated instanton data; the current $\hat{R}_\vartheta$ may be treated analogously. This is preferable to taking numerical derivatives of the Skyrme fields. Fields and currents are generated on a mesh of $50 \times 50 \times 50$ points. However, because of the discrete symmetries (4.2), it is sufficient to compute the fields and currents on a mesh of $25 \times 25 \times 25$ points.

Consider now the calculation of the potential, metric and static deuteron properties from the fields $\hat{U}(\rho, \boldsymbol{x})$ and the currents $\hat{R}_i(\rho, \boldsymbol{x})$ and $\hat{R}_\rho(\rho, \boldsymbol{x})$. It is convenient to define quantities u_0, $\boldsymbol{u}$, $\boldsymbol{a}_i$ and $\boldsymbol{a}_\rho$ via

$$
\begin{aligned}
\hat{U} &= u_0 + i\boldsymbol{u} \cdot \boldsymbol{\tau} \\
\hat{R}_i &= i\boldsymbol{a}_i \cdot \boldsymbol{\tau} \\
\hat{R}_\rho &= i\boldsymbol{a}_\rho \cdot \boldsymbol{\tau},
\end{aligned}
\tag{A.6}
$$

and to introduce the following abbreviations:

$$
\begin{aligned}
\boldsymbol{b}_i &= \epsilon_{ijk} x_j \boldsymbol{a}_k \\
\boldsymbol{f}(\boldsymbol{\alpha}) &= \boldsymbol{u} \times \boldsymbol{\alpha} + u_0 \boldsymbol{\alpha} \\
\boldsymbol{F}(\boldsymbol{\alpha}, \boldsymbol{\beta}) &= \boldsymbol{f}(\boldsymbol{\alpha})(\boldsymbol{u} \cdot \boldsymbol{\beta}) - \boldsymbol{f}(\boldsymbol{\beta}).(\boldsymbol{u} \cdot \boldsymbol{\alpha}).
\end{aligned}
\tag{A.7}
$$

Then the integrand of the potential energy (2.10) takes the form

$$
\boldsymbol{a}_i \cdot \boldsymbol{a}_i + \tfrac{1}{2}((\boldsymbol{a}_i \cdot \boldsymbol{a}_i)(\boldsymbol{a}_j \cdot \boldsymbol{a}_j) - (\boldsymbol{a}_i \cdot \boldsymbol{a}_j)(\boldsymbol{a}_i \cdot \boldsymbol{a}_j)),
\tag{A.8}
$$

and the terms that appear in the integrands of the metric coefficients (5.4) - (5.7) can be written as

$$
\begin{aligned}
\mathrm{tr}(\boldsymbol{x} \times \hat{\boldsymbol{R}})_1^2 &= -2\boldsymbol{b}_1 \cdot \boldsymbol{b}_1 \\
\mathrm{tr}([\tau_1, \hat{U}]\hat{U}^\dagger)^2 &= 8(u_2^2 + u_3^2) \\
\mathrm{tr}([\tau_3, \hat{U}]\hat{U}^\dagger(\boldsymbol{x} \times \hat{\boldsymbol{R}})_3) &= 4if_3(\boldsymbol{b}_3 \times \boldsymbol{u}) \\
\mathrm{tr}\Big([(\boldsymbol{x} \times \hat{\boldsymbol{R}})_1, \hat{\boldsymbol{R}}_i][(\boldsymbol{x} \times \hat{\boldsymbol{R}})_1, \hat{\boldsymbol{R}}_i]\Big) &= -8((\boldsymbol{b}_1 \times \boldsymbol{a}_1)^2 + (x_2^2 + x_3^2)(\boldsymbol{a}_2 \times \boldsymbol{a}_3)^2) \\
\mathrm{tr}\Big([[\tau_1, \hat{U}]\hat{U}^\dagger, \hat{\boldsymbol{R}}_i][[\tau_1, \hat{U}]\hat{U}^\dagger, \hat{\boldsymbol{R}}_i]\Big) &= 32\sum_i(\boldsymbol{a}_i^2(u_2^2 + u_3^2) - f_1^2(\boldsymbol{u} \times \boldsymbol{a}_i)) \\
\mathrm{tr}\Big([[\tau_3, \hat{U}]\hat{U}^\dagger, \hat{\boldsymbol{R}}_i][(\boldsymbol{x} \times \hat{\boldsymbol{R}})_3, \hat{\boldsymbol{R}}_i]\Big) &= -16iF_3(\boldsymbol{a}_i, \boldsymbol{b}_3 \times \boldsymbol{a}_i),
\end{aligned}
\tag{A.9}
$$

together with cyclic permutations.

34

The formula (2.12) for the baryon density $\hat{B}^0(\rho, \boldsymbol{x})$ for fields in standard orientation is now

$$\hat{B}^0 = -\left(\frac{1}{2\pi^2}\right)\boldsymbol{a}_1\cdot\boldsymbol{a}_2 \times \boldsymbol{a}_3, \tag{A.10}$$

and the static deuteron properties may be calculated from the following three moments of the baryon density:

$$I_i(\rho) = \tfrac{1}{2}\int d^3x \; x_i^2 \hat{B}^0(\rho, \boldsymbol{x}), \qquad i = 1, 2, 3. \tag{A.11}$$

Explicitly one finds

$$
\begin{aligned}
r_{\text{rms}}^2 &= I_1 + I_2 + I_3 \\
\hat{Q}_{11} &= 2I_1 - I_2 - I_3 \\
\hat{Q}_{22} &= 2I_2 - I_1 - I_3 \\
\hat{m}_{11} &= \tfrac{1}{2}(I_2 + I_3) \\
\hat{m}_{22} &= \tfrac{1}{2}(I_1 + I_3).
\end{aligned}
\tag{A.12}
$$

All these integrals have to be computed for several values of ρ. The integration over $\mathbf{R}^3$ is facilitated by mapping the whole of $\mathbf{R}^3$ bijectively to the finite cube $C = [-1, 1] \times [-1, 1] \times [-1, 1]$. The mesh used is uniform on C, but the mapping between $\mathbf{R}^3$ and C changes with the Skyrmion separation. In keeping with the earlier discussion, consider coordinates (x_1, x_2, x_3), with respect to which the Skyrmions are separated along the 1-axis. The cube C has coordinates (c_1, c_2, c_3), each taking values in $[-1, 1]$. The form of the mapping is motivated by the observation that at large separations the Skyrmion positions are approximately $(\pm L_1, 0, 0)$ and their size is approximately $\sqrt{L_2 L}$, where L_1 and L_2 are the lengths of the semi-major and the semi-minor axes of the ellipse in the Harthorne data of figure 1. The aim is to concentrate mesh points around the Skyrmion centres, where the integrands make their largest contributions. Explicitly,

$$x_j = \frac{(\kappa\sqrt{L_2 L})c_j}{(1 - c_j)^2} \tag{A.13}$$

for $j = 2, 3$, where κ is a dimensionless parameter that controls the degree to which points are concentrated near the Skyrmion centres; all calculations here had $\kappa = 0.4$. The relation between c_1 and x_1 comes in two parts:

$$x_1 = c_1\left(4L_1(1 - c_1) - (\kappa\sqrt{L_2 L})(1 - 2c_1)\right) \qquad \text{for} \qquad c_1 \in [0, \tfrac{1}{2}) \tag{A.14}$$

and

$$x_1 = \frac{L_1 + \tfrac{1}{4}(\kappa\sqrt{L_2 L})(c_1 - \tfrac{1}{2})}{(1 - c_1)^2} \qquad \text{for} \qquad c_1 \in [\tfrac{1}{2}, 1]. \tag{A.15}$$

The two pieces fit together smoothly at $c_1 = \frac{1}{2}$. The expressions for c_1 negative are chosen so that $x_1(c_1)$ is an odd function.

After the mapping, the integrals are calculated via tricubic interpolation, as in [23]. The factors $(1-c_i)^2$ in the denominators of (A.13) and (A.15) ensure that all the integrands have vanishing gradients at the boundary of C. (The denominator in [23] was simply $(1-c_i)$, which is fine for integrands falling off at least as fast as r^{-6} for large r; here, some of the metric integrals fall off like r^{-4}, and this requires a different power if the tails are to be handled correctly.)

We have computed the integrals (A.8),(A.9),(A.10) and (A.11) for sixteen different values of ρ. The corresponding values for ϑ are all the multiples of $2°$ in the range $2° \leq \vartheta \leq 30°$, and an additional point at $\vartheta = 1°$, included to have a better check against the asymptotic expressions (5.19) - (5.21). The range of values of ρ covered in this way is $[1.71, 15.3]$ (the size of an isolated Skyrmion in these units is ≈ 1). To compute all quantities for each separation takes approximately one hour on a workstation with an R4000 processor. There is good agreement asymptotically with (5.19) - (5.21) and the additional symmetries (5.15) and (5.16) when $\rho = \rho_0$ are also clearly present. The integrated baryon number density never leaves the range $[2.0003, 2.0049]$, and there is no evidence for regions of negative baryon density.

References

[1] T.H.R. Skyrme, Proc.Roy.Soc. **A260** (1961) 127

[2] T.H.R. Skyrme, Nucl.Phys. **B31** (1962) 556

[3] N.S. Manton, Phys.Rev.Lett. **60** (1988) 1916

[4] E. Braaten and L. Carson, Phys.Rev. **D38** (1988) 3525

[5] J.J.M. Verbaarschot, T.S. Walhout, J. Wambach and H.W. Wyld, Nucl.Phys. **A468** (1987) 520

[6] G.S. Adkins, C.R. Nappi and E. Witten Nucl.Phys. **B228** (1983) 552

[7] G.S. Adkins, C.R. Nappi, Nucl.Phys. **B233** (1984) 109

[8] D. Giulini, Mod.Phys.Lett. **A8** (1993) 1917

[9] D. Finkelstein and J. Rubinstein, J.Math.Phys. **9** (1968) 1762

[10] M.F. Atiyah and N.S. Manton, Phys.Lett. **222B** (1989) 430

[11] N.S. Manton, 'Skyrme Fields and Instantons' in : Geometry of Low-dimensional Manifolds (LMS Lecture Notes 150, S.K. Donaldson and C.B. Thomas eds., Cambridge University Press 1990)

[12] M.F. Atiyah and N.S. Manton, Comm.Math.Phys. **153** (1993) 391

[13] A. Hosaka, S.M. Griffies, M. Oka and R.D. Amado, Phys.Lett. **251B** (1990) 1

[14] R. Jackiw, C. Nohl and C. Rebbi, Phys.Rev. **D15** (1977) 1642

[15] B.J. Schroers, Z.Phys. **C61** (1994) 479

[16] L. Landau and E.M. Lifshitz, Quantum Mechanics, 3rd ed. (Pergamon, Oxford, 1977)

[17] E. Witten, Nucl.Phys. **B223** (1983) 422, Nucl.Phys. **B223** (1983) 433

[18] G.W. Gibbons and N.S. Manton, Nucl.Phys. **B274** (1986) 183; B.J. Schroers, Nucl.Phys. **B367** (1991) 177

[19] J.M. Blatt and V.F. Weisskopf, Theoretical Nuclear Physics (Wiley, New York, 1952)

[20] T.E.O. Ericson, Nucl.Phys. **A416** (1984) 281c

[21] T.E.O. Ericson and W. Weise, Pions and Nuclei (Oxford University Press, Oxford, 1988)

[22] A. Jackson, A.D. Jackson and V. Pasquier, Nucl.Phys. **A432** (1985) 567; R. Vinh Mau, M. Lacombe, B. Loiseau, W.N. Cottingham and P. Lisboa, Phys.Lett. **150B** (1985) 259

[23] R.A. Leese and N.S. Manton, Nucl.Phys. **A572** (1994) 575

Note added: N.R. Walet has recently also computed the restriction of the Skyrme Lagrangian to instanton-generated Skyrme fields of degree two (FAU-T3-94/1, hep-ph/9410254). He considered three one-parameter families of such fields, including the attractive channel fields studied here.

Figure Captions

1. The Hartshorne data for instanton-generated two-Skyrmions in the attractive channel. The circle and the ellipse are shown in standard orientation; the isosceles triangle with vertices $X_1 = (0, L, 0, 0), X_2 = (-L \cos \vartheta, -L \sin \vartheta, 0, 0)$ and $X_3 = (L \cos \vartheta, -L \sin \vartheta, 0, 0)$ specifies the JNR data used in our calculations.

2. Spatial moments of inertia.

3. The spatial moment of inertia a^2, shown on a smaller scale than in figure 2.

4. Iso-spatial moments of inertia.

5. The cross term w which couples spin and iso-spin.

6. The radial metric coefficient f^2.

7. The potential V (solid line) and the effective potential V_{eff} (dashed line) which occurs in the radial Schrödinger equation for the deuteron. Both are plotted in geometrical units.

8.a) The radial part u_d of the deuteron wavefunction; for this plot the normalisation is chosen so that $u(\rho_0) = 1$.

8.b) The radial probability distribution $u_d^2 \, abcABCf$ for the deuteron state, normalised so that $\int_{\rho_0}^{\infty} d\rho \, u_d^2 \, abcABCf = 1$.

9.a) Equally spaced density contours for the spatial probability distribution p_d of nuclear matter in the deuteron state Ψ_d. The distribution is axially symmetric about the 3-axis, and shown here in the $x_1 x_3$-plane. Both x_1 and x_3 are measured in fermi.

9.b) Density contours for the spatial probability distribution of the nucleons calculated in a conventional potential model of the deuteron, with the nucleons treated as point-like particles. (From [21], with kind permission of Oxford University Press)
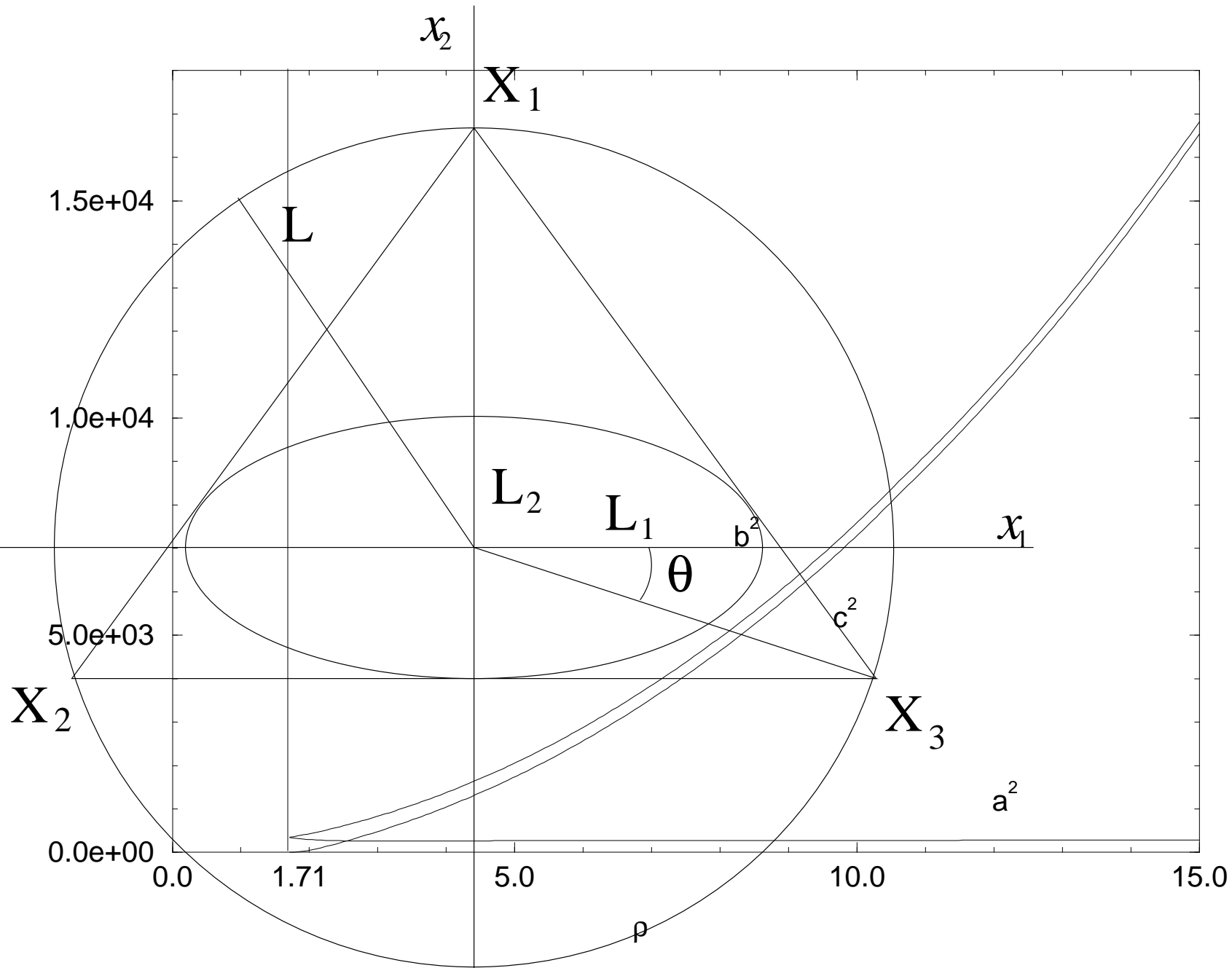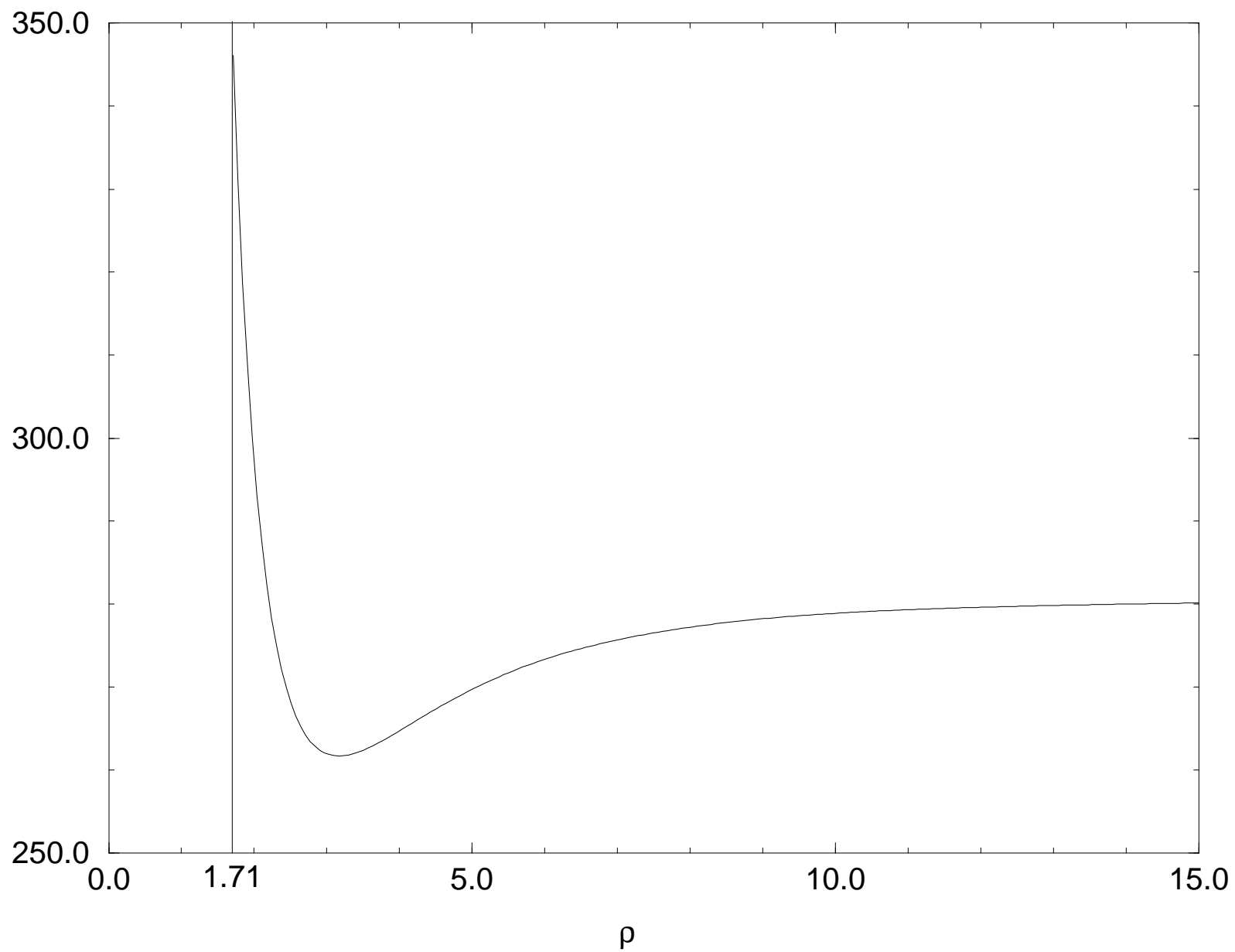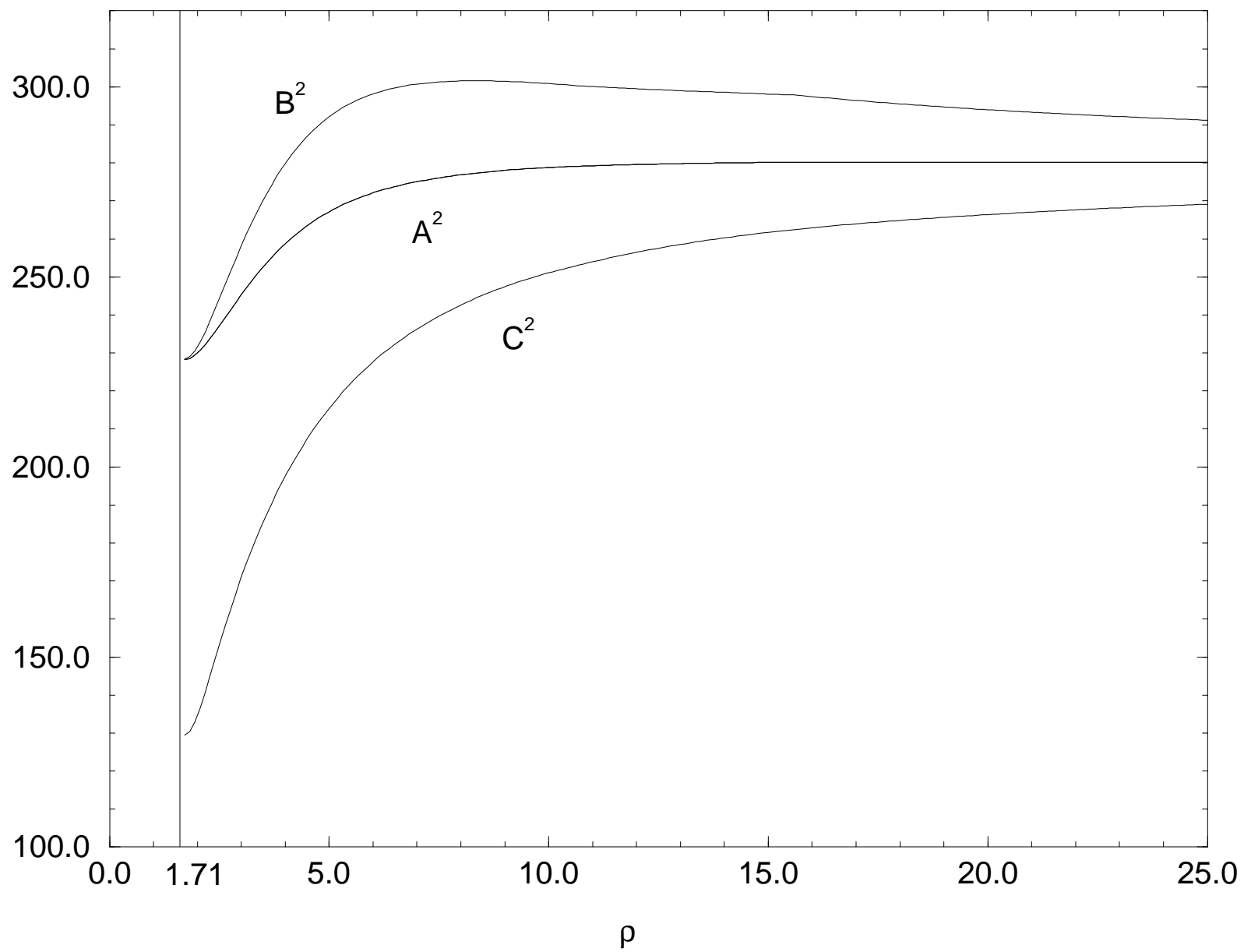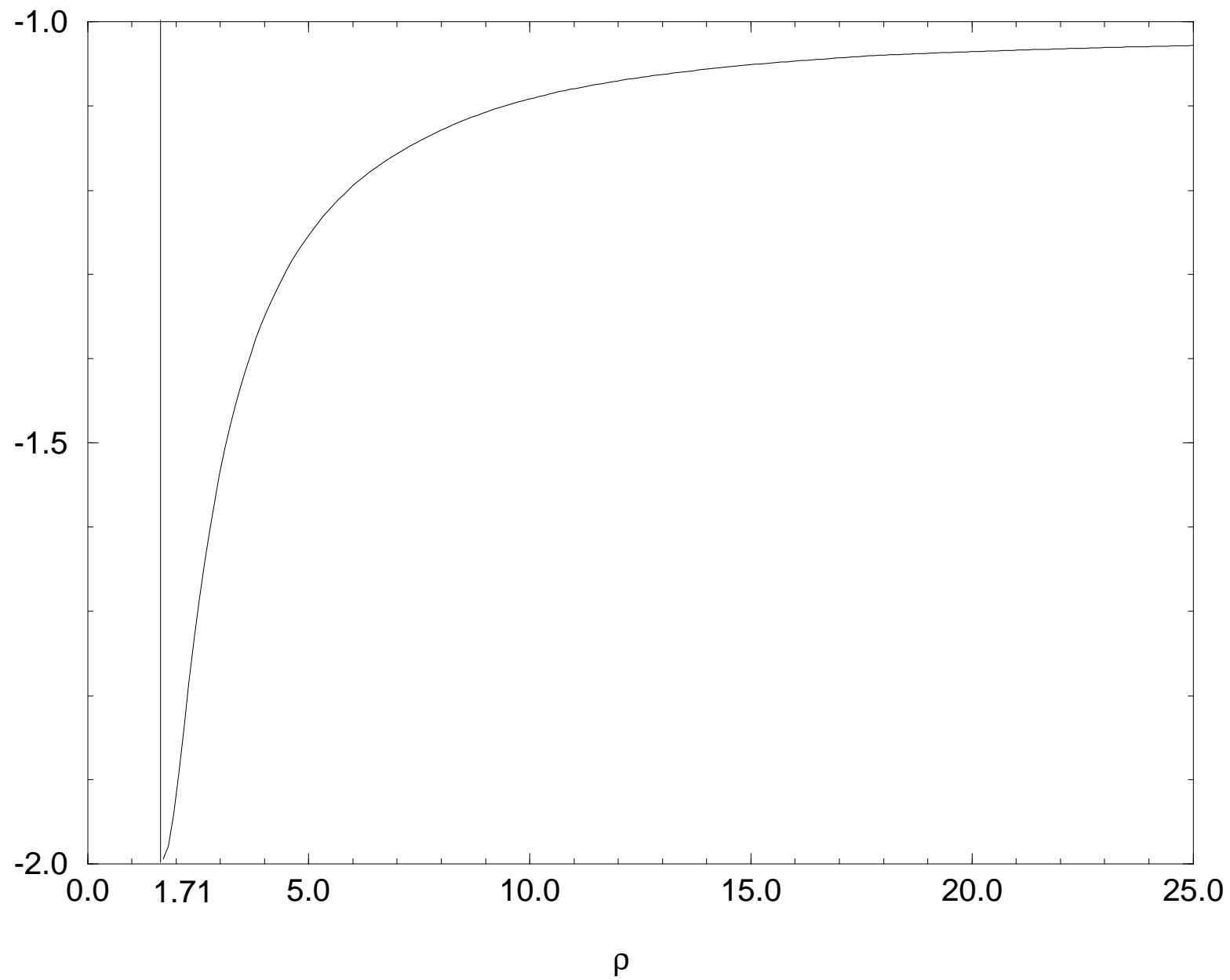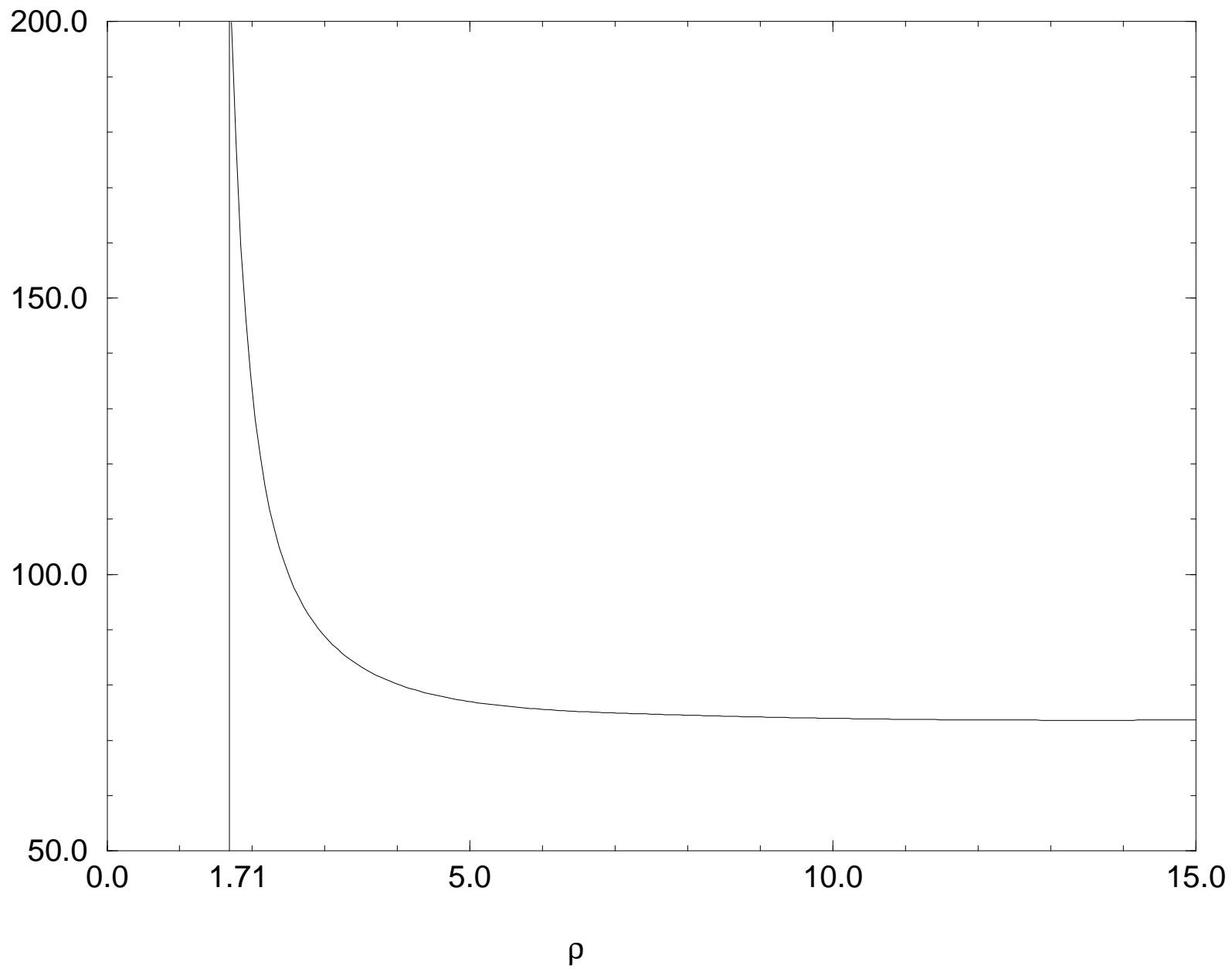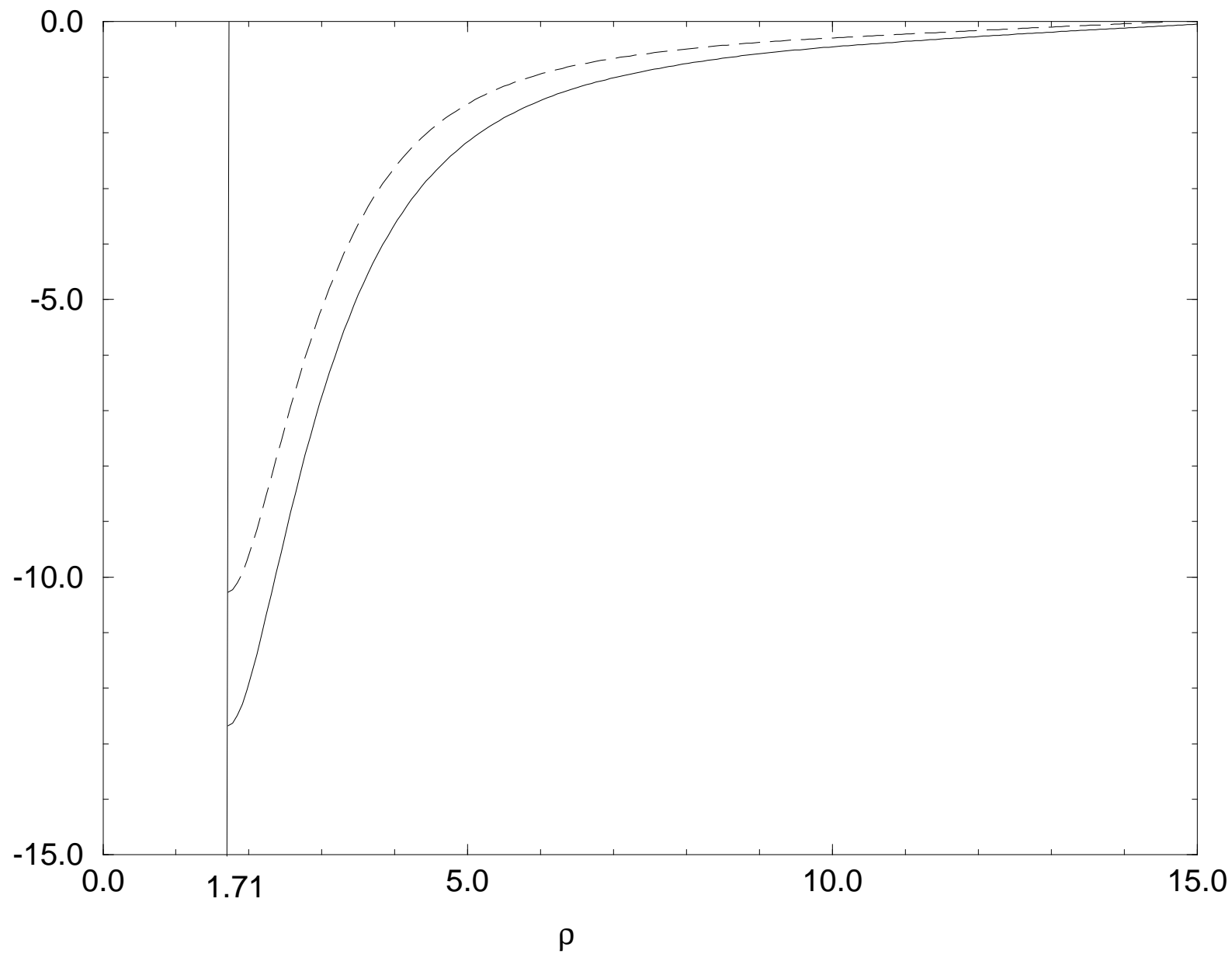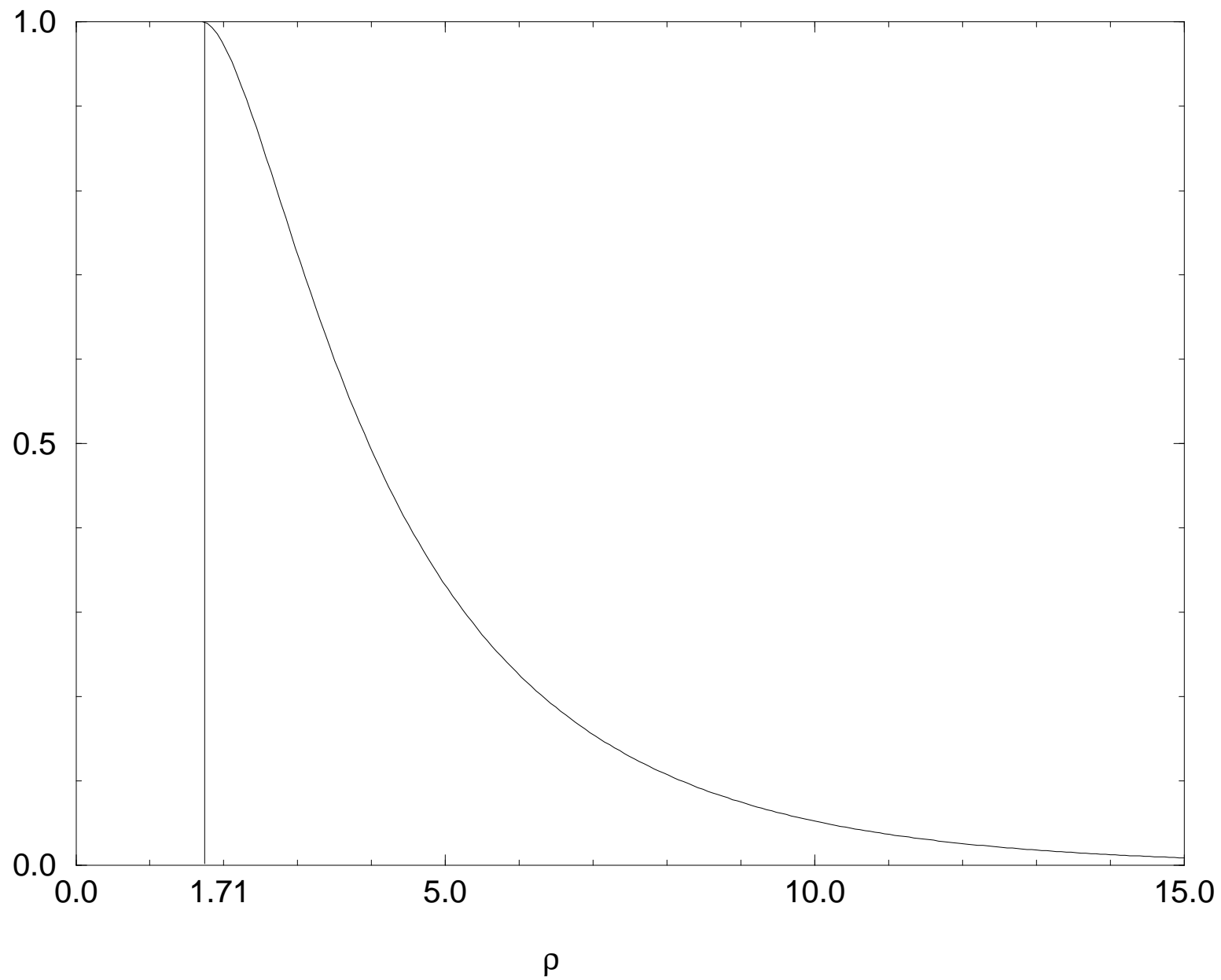
Figure 1

Figure 2

Figure 3

Figure 4

Figure 5

Figure 6

Figure 7

Figure 8.a

Figure 8.b

Figure 9.a

DEUTERON DENSITY CONTOURS